Acta Neuropathologica Communications

RESEARCH

Open Access

Presenilin-dependent regulation of neuronal tau pathology via the autophagy and proteasome pathways

Anna del Ser-Badia[1,2,8†], Carlos M. Soto-Faguás[1,2,9†], Rebeca Vecino[2,3,4], Carles Vendrell[1,2], Laura Molina-Porcel[2,5,6], Raquel Sánchez-Valle[2,5], José Rodríguez-Alvarez[1,2], Carlos Vicario[2,3,4] and Carlos A. Saura[1,2,7*]

Abstract

Mutations in the presenilin (*PS*/*PSEN*) genes cause early-onset familial Alzheimer's disease (AD) by enhancing cerebral accumulation of amyloid-β (Aβ) peptides and microtubule-associated protein tau (MAPT). How PS mutations affect Aβ generation is well characterized, but the precise cellular mechanisms by which PS dysfunction drives neuronal tau pathology are not fully understood. Here, we investigated the mechanisms linking PS/γ-secretase-dependent tau pathology and autophagy/proteasome by employing pathological, imaging and molecular approaches in human brains, fibroblasts and induced pluripotent stem cells (iPSC)-derived neurons from *PSEN1*-linked familial AD carriers, and in a novel neuronal *PS*-deficient tauopathy transgenic mouse. We found enhanced levels and colocalization of pathological phosphorylated tau (pTau) and ubiquitin factor p62 in the hippocampus of dementia patients with familial AD-linked *PSEN1* mutations, corticobasal degeneration and Pick's disease, suggesting disrupted proteasomal degradation in tauopathies. Human primary fibroblasts from *PSEN1* G206D and/or L286P carriers showed elevated LC3-I and autolysosomes indicating autophagy flux alterations. Human iPSC-derived neurons harboring the familial-AD linked *PSEN1* G206D mutation showed increased aggregated tau and reduced secreted tau, whereas pharmacological proteasome inhibition reduced significantly total and pTau (Ser396/404) while increasing its release. Consistently, proteasomal inhibition decreased intracellular tau and pTau and promoted tau release in human tau-expressing neurons through a mechanism that partially depends on PS. In the hippocampus of neuronal *PS*-deficient mice, Akt activation and GSK3β inhibition were associated with elevated levels of phosphorylated and aggregated tau and the ubiquitin-binding protein p62. In conclusion, *PS* function is required for autophagy/proteasome-mediated tau elimination in neurons, whereas that FAD-linked *PSEN1* mutations cause progressive tau pathology by disrupting the proteasome and autophagy/lysosomal pathways.

Keywords Alzheimer's disease, Autophagy, Proteasome, γ-Secretase, Neurodegeneration, Proteostasis, Tauopathies

†Anna del Ser-Badia and Carlos M. Soto-Faguás have contributed equally to this work.

*Correspondence:
Carlos A. Saura
carlos.saura@uab.cat

Full list of author information is available at the end of the article

Background

Alzheimer's disease (AD), the most prevalent memory disorder in the elderly, is characterized by cerebral accumulation of amyloid plaques, containing amyloid-β (Aβ) peptides, and neurofibrillary tangles (NFTs) of aggregated hyperphosphorylated microtubule-associated protein tau (MAPT) [1, 2]. Tau pathology progresses in a stereotypical manner between interconnected brain regions, appearing in the transentorhinal/entorhinal cortex and hippocampal region, then spread to limbic and finally association neocortex , which correlates with the progression and severity of the disease [3, 4]. Elevated levels of phosphorylated tau (pTau) species in brain and plasma are associated with cognitive decline and conversion to dementia, making them potentially useful biomarkers for clinical diagnosis [5–8].

The majority of familial AD (FAD) cases are caused by autosomal dominant mutations in the *presenilin* (*PS/PSEN*) genes (presenilin-1/2: *PSEN1*, *PSEN2*), encoding the catalytic components of γ-secretase [9]. These pathogenic mutations increase the accumulation of toxic Aβ peptides and hyperphosphorylated tau, causing accelerated disease progression [10–13]. Although Aβ and tau act synergistically in AD [14–16], tau also causes neurodegeneration independently of Aβ [17], as evidenced in primary tauopathies, such as corticobasal degeneration (CBD), Pick's disease (PiD) and progressive supranuclear palsy (PSP) [18]. In rare cases of familial frontotemporal dementia, atypical dementia with parkinsonism and dementia with Lewy bodies, *PSEN1* mutations enhance tau accumulation independently of Aβ [19–22]. FAD-linked *PSEN* mutations also increase tau phosphorylation, amyloid deposition, synaptic dysfunction and neurodegeneration in mice [23–25]. These mutations interfere with γ/ε-secretase-dependent and -independent PS biological functions revealing a possible loss of function mechanism [26]. Consistently, PS deficiency in neurons results in age-dependent synaptic dysfunction and neurodegeneration accompanied by tau phosphorylation in *PS* conditional knockout (cKO) mice [27–29]. Although loss of PS/γ-secretase recapitulates key features of tauopathies, the PS-dependent mechanisms leading to tau pathology in neurons during neurodegeneration are still unknown.

Macroautophagy, hereafter referred as autophagy, is a catabolic cellular process that targets proteins and organelles to autophagosomes for degradation, and plays a central role in neurodegenerative diseases, including tauopathies [30]. The accumulation of autophagic vesicles is associated with neurofibrillary pathology in AD, CBD and PSP cases, which suggests disruption of autophagy-lysosomal degradation in tauopathies [31–33]. Pathological tau disrupts both autophagy and chaperone-mediated autophagy (CMA), contributing to proteostasis imbalance and neurotoxicity in AD [34–36]. Conversely, autophagy activation potentiates the clearance of toxic protein aggregates containing tau and Aβ [36–43]. Synaptic activity also decreases pathological tau by promoting its degradation via the autophagy/lysosomal pathway and increasing its extracellular release [44–46]. Alongside the autophagy-lysosomal pathway, the ubiquitin-proteasome system (UPS) plays a major role in the clearance of intracellular tau, although the predominant degradation mechanism may depend on the tau protein species [47]. PS1 promotes autophagy-mediated proteolysis by facilitating autophagosome-lysosome fusion, autophagy-related genes and lysosome acidification [48–56]. Besides the critical role of PS in autophagy (see [57] for a review), whether PS regulates autophagy- and/or proteasome-mediated tau clearance during neurodegeneration is still unclear. Here, we investigated the cellular mechanisms of PS-dependent tau pathology by examining the link between tau and autophagy and proteasome degradation in human brains, iPSC-derived neurons and primary fibroblasts from FAD-linked *PSEN1* carriers, as well as in novel mouse models of tauopathy lacking neuronal PS genes.

Materials and methods

Human brain samples

Human post-mortem hippocampus from controls (n = 14), FAD-linked *PSEN1* (n = 6) and *PSEN2* (n = 1) carriers, CBD (n = 8) and PiD (n = 7) were obtained from the Neurological Tissue Bank, Biobanc Hospital Clínic-FRCB/IDIBAPS, and Banc de Teixits de Bellvitge (Barcelona, Spain). Control brain samples were obtained from patients who died from non-neurological diseases; diagnostic neuropathology and retrospective chart reviews were carried out for all subjects (Table 1). Neuropathology was classified according to the ABC score that includes the distribution of Aβ deposits according to Thal phases (A), Braak staging for neurofibrillary pathology (B) and the frequency of cortical neuritic plaques according to CERAD criteria (C) [58]. All procedures were approved by the Human Ethical Committee of Hospital Clinic. All patients' data and samples were coded and handled according to national guidelines to protect patients' identities.

Transgenic mice

PS cKO mice (C57BL/6/129 background) lacking *PS1* and *PS2* specifically in forebrain glutamatergic neurons were previously described [27]. Littermate control (*PS1* f/f; $PS2^{+/+}$ or *PS1* f/f; $PS2^{+/-}$; f: floxed), PS1 cKO (*PS1* f/f; CaMKIIα-Cre) and PS cKO (*PS1* f/f; $PS2^{-/-}$; CaMKIIα-Cre) mice were obtained by crossing floxed *PS1*/$PS2^{-/-}$ (*PS1* f/f; $PS2^{-/-}$) or $PS2^{+/-}$ (*PS1* f/f; $PS2^{+/-}$) males to heterozygous PS1 cKO; $PS2^{+/-}$ females (*PS1* f/f; $PS2^{+/-}$;

Table 1 Pathological characteristics of human hippocampal samples of this study

Sample ID	Gender	Age disease-onset	Age	Clinical Diagnosis	Thal stage	Braak stage	CERAD	ABC score	α-synuclein pathology	APOE status	PMD (h: min)	BC	IHC	AV
CTRL 1	F	N/A	64	Control	–	NFT scant	–	–	–	Unknown	5:00	✓		
CTRL 2	F	N/A	46	Control	–	–	–	–	–	Unknown	9:35	✓		
CTRL 3	F	N/A	55	Control	–	NFT scant	–	–	–	Unknown	8:30	✓		
CTRL 4	M	N/A	43	Control	–	–	–	–	–	Unknown	4:35	✓		
CTRL 5	M	N/A	56	Control	–	NFT scant	–	–	–	Unknown	5:00	✓		
CTRL 6	M	N/A	52	Control	–	–	–	–	–	Unknown	3:00	✓		
CTRL 7	M	N/A	44	Control	–	–	–	–	–	Unknown	6:40	✓		
CTRL 8	M	N/A	78	Control	5	V	Moderate	A3B3C2	–	Unknown	5:00		✓	✓
CTRL 9	F	N/A	83	Control	5	II	Moderate	A3B1C2	–	ε3/ε4	7:33		✓	
CTRL 10	M	N/A	86	Control	3	II	Sparse	A2B1C1	Brainstem LBD (Braak 1)	ε3/ε3	7:25		✓	✓
CTRL 11	M	N/A	94	Control	5	II	Moderate	A3B1C2	–	ε3/ε3	15:46		✓	✓
CTRL 12	F	N/A	77	Control	5	V	Moderate	A3B3C2	–	Unknown	4:30			✓
CTRL 13	F	N/A	93	Control	4	II	Moderate	A3B1C2	–	ε3/ε3	13:40			✓
CTRL 14	F	N/A	90	Control	3	III	Moderate	A2B2C2	–	ε3/ε3	12:20			✓
FAD 1	F	47	56	FAD *PSEN1* P264L	5	VI	Frequent	A3B3C3	–	ε4/ε4	6:00	✓	✓	✓
FAD 2	F	39	48	FAD *PSEN1*M139T	5	VI	Frequent	A3B3C3	Amygdala predominant LBD	Unknown	16:41	✓	✓	✓
FAD 3	F	45	61	FAD *PSEN2* R62H	5	VI	Frequent	A3B3C3	–	Unknown	7:00	✓	✓	✓
FAD 4	F	42	53	FAD *PSEN1* L286P	5	VI	Frequent	A3B3C3	–	ε3/ε3	7:15	✓	✓	✓
FAD 5	M	48*	57	FAD *PSEN1*M139T	5	VI	Frequent	A3B3C3	–	ε3/ε3	15:25	✓	✓	✓
FAD 6	M	35*	44	FAD *PSEN1*E120G	5	VI	Frequent	A3B3C3	–	ε3/ε3	5:30	✓	✓	✓
FAD 7	M	46*	53	FAD *PSEN1*M139T	5	VI	Frequent	A3B3C3	Limbic LBD	ε2/ε3	5:25	✓	✓	✓
CBD 1	F	58	69	CBD	1	0	None	A1B0C0	–	Unknown	12:10	✓	✓	
CBD 2	F	74	79	CBD	4	IV	Moderate	A3B2C2	–	Unknown	10:30	✓	✓	
CBD 3	F	63	67	CBD	3	0	Sparse	A2B0C1	–	Unknown	6:45	✓	✓	
CBD 4	F	75	78	CBD	4	II	Moderate	A3B1C2	–	ε3/ε4	5:30	✓	✓	
CBD 5	M	65	74	CBD	3	0	Sparse	A2B0C1	–	Unknown	14:30	✓	✓	
CBD 6	M	72	72	CBD	0	0	None	A0B0C0	–	Unknown	7:00	✓	✓	
CBD 7	M	Unknown	66	CBD	0	0	None	A0B0C0	–	Unknown	–	✓	✓	

Table 1 (continued)

Sample ID	Gender	Age disease-onset	Age	Clinical Diagnosis	Thal stage	Braak stage	CERAD	ABC score	α-synuclein pathology	APOE status	PMD (h: min)	BC	IHC	AV
CBD 8	M	51	59	CBD	0	0	None	A0B0C0	–	ε3/ε3	7:00	✓		
PiD 1	F	33	41	PiD	1	0	None	A1B0C0	–	Unknown	11:10	✓		
PiD 2	F	64*	75	PiD	3	III	Moderate	A2B2C2	–	Unknown	13:00	✓		
PiD 3	F	61	69	PiD	3	0	Sparse	A2B0C1	–	Unknown	3:00	✓	✓	
PiD 4	M	66*	74	PiD	3	0	Frequent	A2B0C2	–	Unknown	13:00	✓	✓	
PiD 5	M	67	73	PiD	5	III	Moderate	A3B2C2	–	Unknown	9:15	✓	✓	
PiD 6	M	60	78	PiD	1	0	None	A1B0C0	–	Unknown	11:00	✓	✓	
PiD 7	F	59	70	PiD	1	0	None	A1B0C0	–	Unknown	5:45		✓	

Samples are classified according to the clinical and neuropathological diagnosis.

FAD, familial Alzheimer's disease; CBD, corticobasal degeneration; PiD, Pick's disease; LBD, lewy body disease; F, female; M, male; CAA, cerebral amyloid angiopathy; CVD, cerebrovascular disease; PMD, postmortem delay; BC, samples used for biochemistry experiments; IHC, samples used for immunohistochemistry experiments; AV, samples used for autophagic vesicles isolation experiments. N/A, not applicable; '–' means not detected; *Age when diagnosed

CaMKIIα-Cre). Novel non-transgenic control (*PS1* f/f; Tau-) and human tau (*PS1* f/f; Tau+), PS1 cKO; Tau (*PS1* f/f; CaMKIIα-Cre; Tau+) and PS cKO; Tau (*PS1* f/f;*PS2*$^{-/-}$; CaMKIIα-Cre; Tau+) mice were obtained by crossing PS1 cKO or PS cKO with Tau P301S tg (PS19) mice (JAX #008169; B6C3). Tau P301S mice express the tau gene with one N-terminal insert and four microtubule binding repeats (1N4R) harboring the FTDP-17-linked P301S mutation under the neuron-specific prion protein promoter (*PrP*) leading to pTau and neurofibrillary tangles and behavior alterations [59]. Animal procedures were conducted in accordance with the reduction principle of the 3Rs following protocols approved by the Animal and Human Ethical Committee of the Universitat Autònoma de Barcelona and Generalitat de Catalunya (CEEAH 2895/ DMAH 10571) based on European Union guidelines and regulations (2010/63, 2016/679).

Primary mouse neurons and human fibroblast cultures

Cortical neurons from Tau (*PS1* f/f;*PS2*$^{+/+}$;Tau+) or PS1 cKO; Tau ((*PS1* f/f;*PS2*$^{+/+}$;Tau) and PS cKO; Tau (*PS1 f/f*;*PS2*$^{-/-}$;Tau+) embryos (E15.5) were cultured in poly-D-lysine coated dishes containing neurobasal medium supplemented with B27 and glutamine (Life Technologies). Neurons (4 DIV) were transduced with lentivirus containing Cre-recombinase and ΔCre-recombinase (control) as reported [60], and then lysed (12 DIV) with cold RIPA-DOC buffer (50 mM Tris HCl, pH 7.4, 150 mM sodium chloride, 0.1% SDS, 1% NP-40, 0.5% sodium deoxycholate, 2.5 mM EDTA, 1 mM Na_3VO_4, 25 mM NaF). Primary human fibroblasts from skin biopsies of healthy and FAD *PSEN1* subjects [61] were transiently transfected (48 h) with the pCDH-EF1a-mCherry-EGFP-LC3B plasmid (Addgene) using Lipofectamine 2000 reagent (Thermo Fisher Scientific). Cells were fixed with phosphate-buffered paraformaldehyde (PFA, 4%) and imaged with a Zeiss Axio Examiner LSM700 laser scanning microscope. ImarisColoc tool from Imaris 8.3.4 (Bitplane) software was used to discriminate between autophagosomes (mCherry- and EGFP-positive) and autolysosomes (mCherry-positive). For pharmacological treatments, cells were incubated with vehicle, chloroquine (10 μM, 24 h; Sigma-Aldrich) and/or MG132 (1 μM, 24 h; Tocris). Cell viability was assessed using the non-toxic PrestoBlue™ assay (ThermoFisher Scientific, A13262).

Quantification of extracellular human tau

Total human tau in the medium of cultured cortical neurons was quantified using a solid phase ELISA kit (KHB0041, Invitrogen). Briefly, the medium was harvested, centrifuged and the supernatant incubated with the capture antibody. Then, samples were incubated with human tau biotin conjugate antibody and streptavidin-HRP solution. After the addition of the chromogen solution, absorbance at 450 nm was measured on a Varioskan™ Lux reader (Thermo Scientific).

Differentiation of human iPSCs into hippocampal neurons

Human iPSCs were obtained by reprogramming dermal fibroblasts isolated from skin biopsies of FAD patient carrying the G206D mutation in the *PSEN1* gene and healthy subjects [61, 62]. The human iPSCs were grown on vitronectin and treated with small molecules LDN 193, 189 and A83-01 (Miltenyi Biotec) to induce a neural cell fate as well as with cyclopamine (Stem cell) to inhibit the sonic hedgehog signalling pathway and promote a telencephalic dorsal phenotype. Neural progenitor cells (NPCs) were expanded by adding FGF-2 (Peprotech) and then were seeded at 300,000 cells/cm^2 in polyornithine (Sigma) and laminin-treated plates (ThermoFisher). Wnt3a, BDNF, NT-3 (Peprotech) and cAMP (Sigma) were added to promote the generation and differentiation of hippocampal neurons, which were cultured for 60 DIV.

Brain fractionation and purification of autophagic fractions

For purification of soluble and insoluble cell fractions, frozen human hippocampi were homogenized in cold detergent-free RIPA-DOC buffer (0.01 g tissue/100 μl) using a Dounce homogenizer (40 strokes), briefly sonicated and centrifuged at 14,000 rpm for 15 min to obtain soluble (supernatant) and insoluble (pellet) fractions, the latter resuspended in RIPA-DOC buffer. Purification of autophagic fractions from brain samples was performed using a self-established modified protocol originally described for liver [63]. Briefly, human hippocampal tissue (0.1 g) was homogenized in ice-cold 0.25 M sucrose with a Teflon-glass homogenizer and centrifuged 5 min at 2000 x *g*. The supernatant was centrifuged 12 min at 17,000 x *g* and the resulting pellet, which contains the enriched autophagic fractions, was resuspended in 0.25 M sucrose and 51% Nycodenz (ProteoGenix). A 26%, 24%, 20% and 15% discontinuous Nycodenz gradient was loaded on top of the sample layer, and centrifuged 3 h at 104,300 x *g*. The autophagosome, autolysosome and lysosome fractions were collected from the 15%-20%, 20%-24% and 24%-26% Nycodenz interphases, respectively. Each fraction was diluted with ice-cold 0.25 M sucrose and centrifuged 1 h at 30,000 x *g*. The pellets with the enriched vesicle fractions were resuspended in RIPA-DOC buffer for characterization by biochemical analysis (Supl Fig. 1C).

Biochemical analysis

For biochemical analysis, hippocampal tissue was lysed in cold-lysis buffer (62.5 mM Tris hydrochloride, pH 6.8, 10% glycerol, 5% β-mercaptoethanol, 2.3% sodium dodecyl sulfate [SDS], 5 mM NaF, 100 μM Na_3VO_4, 1 mM

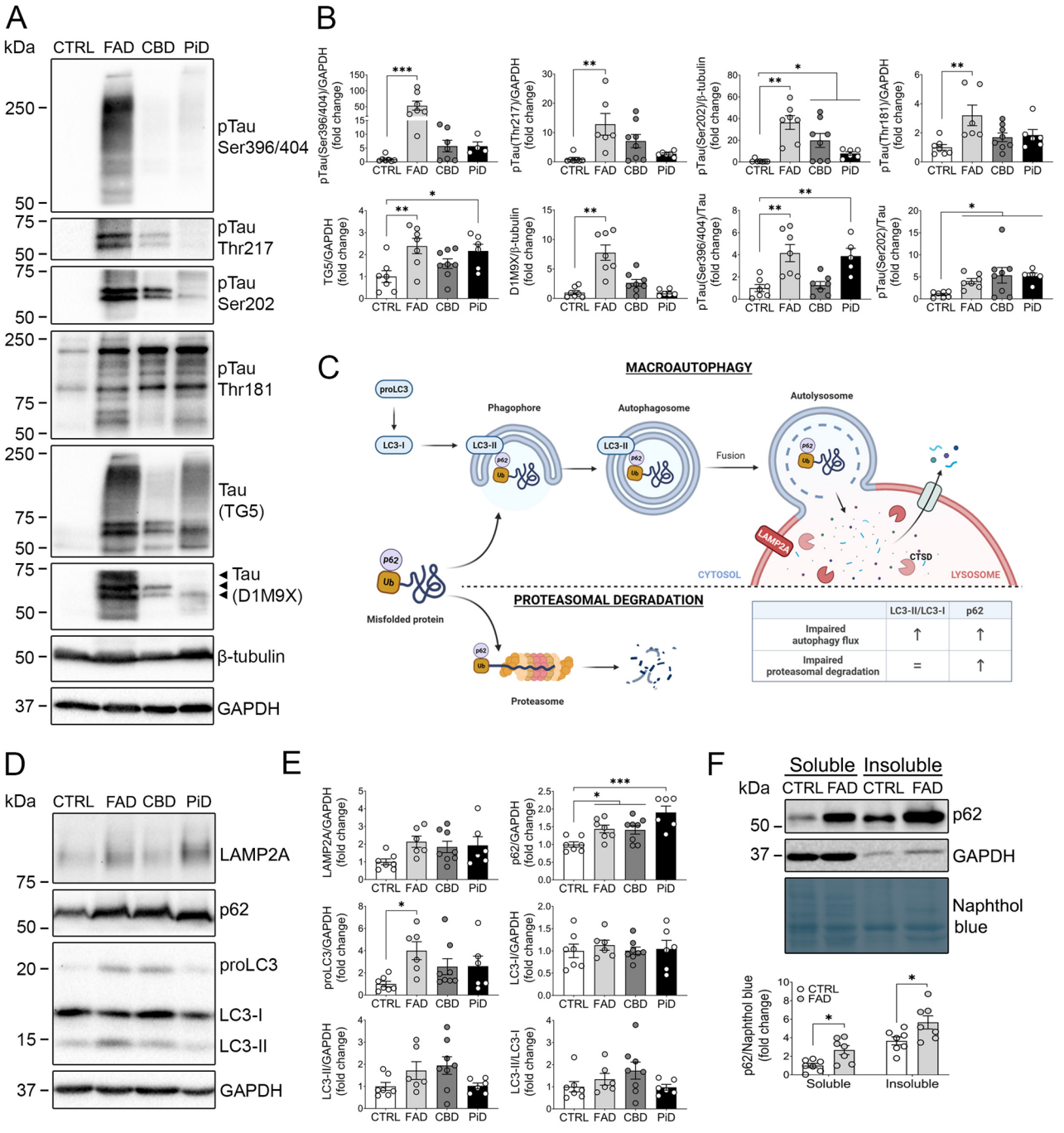

Fig. 1 Increased p62 levels are associated with accumulation of total and phosphorylated tau in the hippocampus of tauopathy patients. **A**,**B**, Western blot and quantification of phosphorylated (p) Ser 396/404 (PHF-1), Thr 217, Ser 202 (CP13) and Thr 181 (AT270) and total (TG5 and D1M9X) tau in hippocampal lysates from controls (CTRL) and patients with FAD, CBD and PiD. Arrowheads indicate ~64, 68 and 72 kDa tau bands. Protein levels were normalized to β-tubulin, GAPDH or total tau (D1M9X antibody). **C**, Scheme of macroautophagy and proteasomal degradation pathways. Misfolded ubiquitinated proteins are recognized by the adaptor protein p62 and can then be either recruited to forming phagophores for lysosomal degradation or directed to the proteasome for degradation. The table shows the expected molecular markers that accumulate when autophagy or proteasome degradation are blocked. **D**, **E**, Biochemical analysis of autophagic/lysosomal markers LAMP2A, p62 and LC3 in hippocampal lysates from controls (CTRL) and patients with FAD, CBD and PiD. **F**, p62 levels in soluble and insoluble hippocampal fractions of controls (CTRL) and FAD-linked PSEN1 patients. Naphtol blue was used as a loading control. Representative hippocampal cases (Table 1) in **A**–**B**, **D**–**E**: CTRL 5, FAD 7, CBD 6 and PiD 3, and in F: CRTL2 and FAD6. Data represent mean ± SEM of multiple individuals (n = 6–8) per group. One-way (**B**,**E**) or two-way (**F**) ANOVA followed by Dunnett's post hoc test was used as statistical test. *$P < 0.05$, **$P < 0.01$, ***$P < 0.001$. CTRL: control; FAD: familial Alzheimer's disease; CBD: corticobasal degeneration; PiD: Pick's disease; Ub: ubiquitin; CTSD: cathepsin D

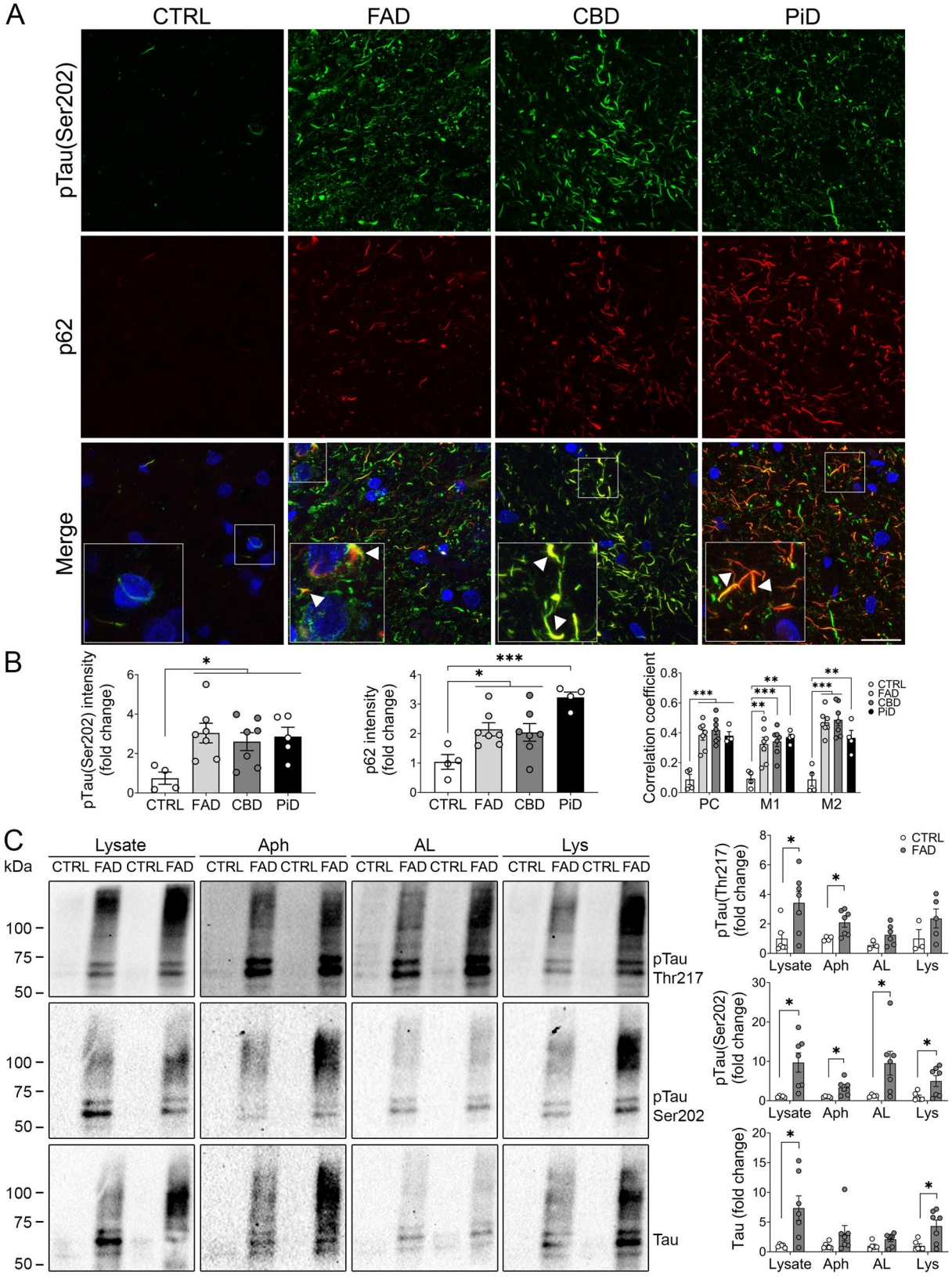

Fig. 2 (See legend on next page.)

(See figure on previous page.)

Fig. 2 Phosphorylated tau accumulates in autophagic vesicles of hippocampus of tauopathy patients. **A**,**B**, Immunofluorescence images of pSer202 Tau (CP13, green) and p62(red), using Fab anti-mouse blocking, in human hippocampal sections of CTRL 10, FAD 1, CBD 4 and PID 6 cases (**A**), and quantitative analyses of total intensity per area and colocalization of pSer202 Tau and p62 (**B**). Data represent mean ± SEM of multiple individuals ($n = 4–7$) per group. Scale bar: 20 µm. One-way ANOVA followed by Dunnett's post hoc test. **C**, Western blot images and quantification analyses of pTau (Thr 217 and Ser 202) and total tau (D1M9X) in lysates and purified enriched autophagosomal (Aph), autolysosomal (AL) and/or lysosomal (Lys) fractions from hippocampus of human CTRL and FAD patients. Representative images corresponding to CTRL 13, CTRL 14, FAD 2 and FAD 7. Welch's t test or Mann-Whitney test were used as statistical test. *$P < 0.05$, **$P < 0.01$, ***$P < 0.001$. CTRL: control; FAD: familial Alzheimer's disease; CBD: corticobasal degeneration; PiD: Pick's disease; PC: Pearson's correlation coefficient; M1/M2: Mander's overlap coefficient 1 and 2

EDTA, 1mM ethylene glycol tetraacetic acid) containing protease and phosphatase inhibitors and boiled at 100 °C. The protein content in lysates and purified enriched fractions was quantified with the Coomassie (Bradford) assay kit (Thermo Fisher Scientific), and same amount of protein per sample was resolved on SDS-polyacrylamide gel electrophoresis and detected by Western blotting with the following antibodies: rabbit anti-tau (D1M9X; 1:1000, Cell Signaling), mouse anti-tau (TG5; 1:500), mouse pThr 181 (AT270; 1:200, Thermo Fisher Scientific), pSer202 (CP13; 1:250) and pSer 396/404 (PHF-1; 1:250) tau, rabbit pThr 217 tau (1:1000, Thermo Fisher Scientific), rabbit anti-LC3B (1:1000, Abcam), mouse anti-p62/SQSTM1 (1:1000, Abcam) and ubiquitin (1:1000; P4D1 Santa Cruz Biotechnology), rabbit anti-LAMP2A (1:1000, Abcam), rabbit anti-Cathepsin D (1:1000, Abcam), rabbit anti-PS1 NTF (1:10000, Calbiochem), mouse anti-β-tubulin (1:20000, Sigma), mouse anti-GAPDH (1:100000; Ambion), mouse anti-GSK3β (1:2500; BD Biosciences), rabbit pGSK3β (Ser 9, 1:1000; Cell Signaling), goat anti-Akt (1:1000; Santa Cruz Biotechnology), and rabbit pAkt (Thr 308 and Ser 473), total and pThr 172 AMPK, total and pSer 2448 mTOR, pPRAS40 Thr 246, total and pThr 389 p70 S6K, total and pSer 235/236 S6 ribosomal protein and pULK1 Ser 757 (all 1:1000, Cell Signaling). Bands detected with secondary antibodies coupled to peroxidase and enhanced chemiluminescent reagent were captured in a ChemiDoc MP System and quantified in a linear range using the ImageLab 5.2.1 software (Bio-Rad).

Immunohistochemistry and Gallyas staining

Mice were perfused transcardially with PBS and fixed in 4% phosphate-buffered PFA before paraffin embedding. Sagittal brain section (5 µm) were deparaffinized in xylene, rehydrated and microwave heated in citrate buffer (10 mM, pH 6.0). Sections were incubated overnight at 4 °C with pSer202 tau antibody (CP13, 1:50). Sections were then incubated with a biotin-conjugated anti-mouse secondary antibody (1:200) and revealed with the DAB peroxidase substrate kit (Vector laboratories) before imaging (Nikon Eclipse 80i microscope). For immunofluorescence staining of human hippocampus, frozen human samples (10 µm) were fixed in 4% PFA and heated in citrate buffer. Sections were incubated overnight at 4 °C with mouse anti-phosphorylated tau (CP13, 1:50), mouse anti-p62 (1:200) or rabbit anti-LC3 (1:200) antibodies followed by anti-mouse AlexaFluor488 (1:300), biotin-conjugated Fab anti-mouse or rabbit antibodies (1:300), Streptavidin Cy3 (1:1000) and Hoechst (1:10,000). Sections were incubated with Sudan Black B and mounted before confocal images (63x) were obtained Confocal images (63x;) were obtained with a Zeiss Axio Examiner LSM700 laser. For Gallyas staining, deparaffinized brain sections were treated with 0.3% $KMnO_4$ (10 min), 1% oxalic acid (1 min) and washed with H_2O_d to stain NFTs [64]. After alkaline silver iodide treatment (1 min), sections were washed (x 3) with 0.5% acetic acid and developed (6–7 min) with solution A (0.2% silver nitrate, 0.2% ammonium nitrate, 1% g tungstosilicic acid and 0.2% formaldehyde) and solution B (5% anhydrous sodium carbonate). Sections were washed (x3) in 1% acetic acid and stained with 0.5% gold chloride. All immunohistochemistry images were analyzed using ImageJ software (NIH). For pTau (Ser 202) and p62 colocalization analysis, Just Another Colocalization plugin (JACoP) was used.

Statistical analysis

Statistical analysis with Prism software (GraphPad, La Jolla, CA) was performed using one- or two-way ANOVA followed by Dunnett's, Tukey's or Bonferroni's *post hoc* test as indicated in the figure legend. For data that did not follow a normal distribution, Kruskal-Wallis followed by Dunn's *post hoc* test was used. *P* values less than 0.05 were considered significant. The significance level is indicated as follows: * $P < 0.05$, ** $P < 0.01$ and *** $P < 0.001$.

Results

Pathological tau accumulates in autophagic vesicles in the hippocampus of FAD subjects

To investigate the link between tau accumulation and protein degradation dysfunction in tauopathies, we first analyzed biochemically total and phosphorylated (Thr 181, Ser 202, Thr 217, Ser 396/404) tau in the hippocampus of 28 individuals clinically diagnosed with *PSEN*-linked FAD (FAD; $n = 7$, mean age: 53.1 ± 5.7), CBD ($n = 8$, mean age: 70.5 ± 6.7), PiD ($n = 6$, mean age: 68.6 ± 12.5) and age and sex-matched controls ($n = 7$, mean age: 51.4 ± 7.6) (Table 1; Fig. 1A, B). Biochemical analysis of tau revealed protein bands of ~60–64, 68 and 72 kDa in FAD samples, whereas 64–68 and 60–64 kDa tau species were predominant in CBD and PiD, respectively (Fig.

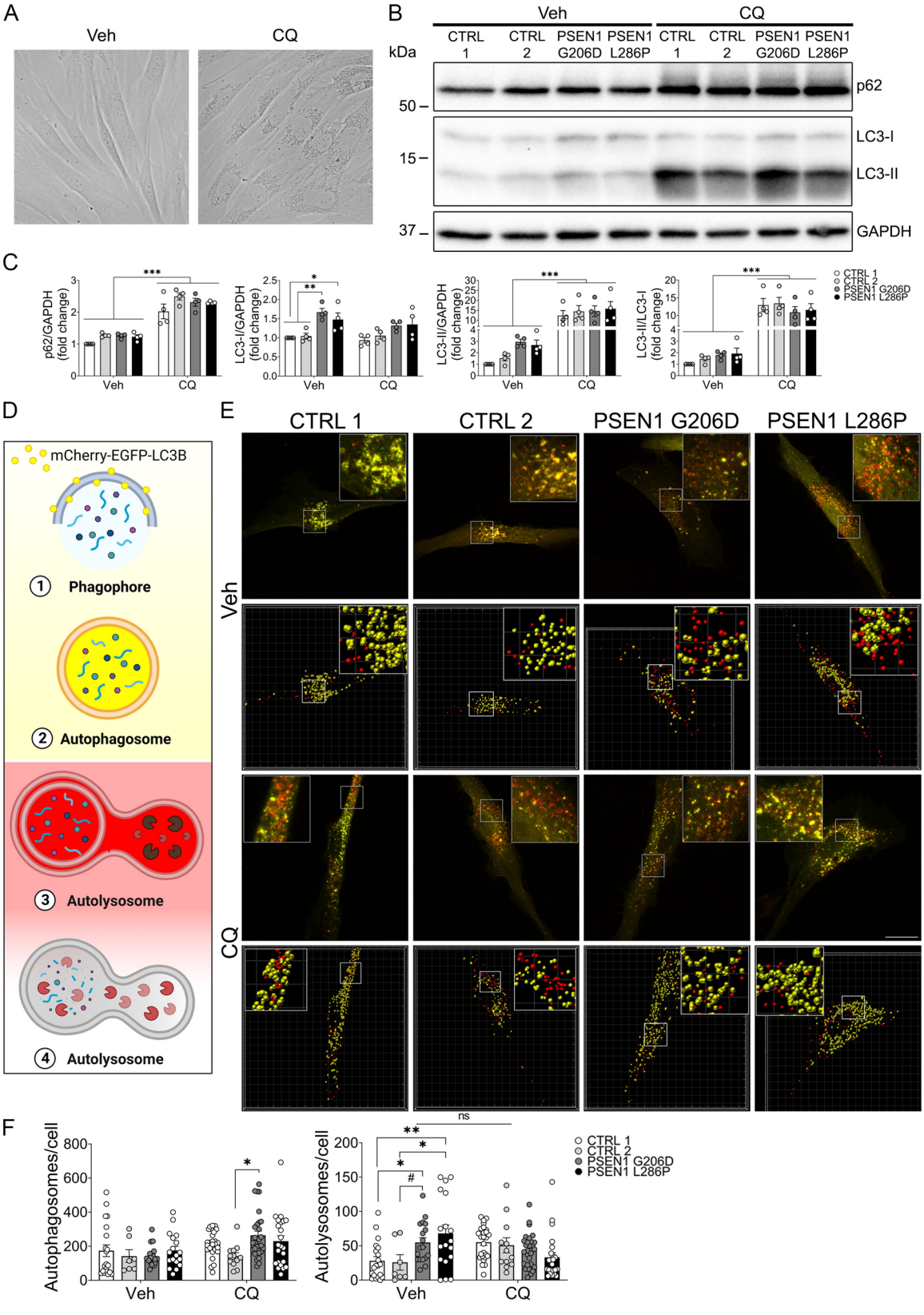

Fig. 3 (See legend on next page.)

(See figure on previous page.)

Fig. 3 FAD-linked PSEN1 G206D and L286P mutations impair autolysosomes clearance in primary human fibroblasts **A**, Representative bright field images of primary human fibroblasts treated with vehicle or CQ. **B**, **C**, Western blotting (**B**) and quantitative analysis (**C**) of p62, LC3-I and LC3-II protein levels in lysates of cultured human fibroblasts treated with vehicle or CQ for 24 h. Protein levels were normalized to GAPDH or LC3-I, as indicated. Data are mean ± SEM of independent cultures (n = 4). Two-way ANOVA followed by Tukey's post hoc test was used as a statistical test. *P < 0.05, **P < 0.01, ***P < 0.001. **D**, Scheme of the autophagy tandem sensor mCherry-EGFP-LC3B. Autophagosomes are labelled in yellow due to mCherry/EGFP co-staining, and after fusing with lysosomes EGFP is quenched by the acidic pH and autolysosomes are labelled in red (mCherry+). **E**, **F**, Confocal microscopy (first and third rows) and Imaris software (second and fourth rows) images (**E**) and quantitative analysis (**F**) of autophagosomes (yellow puncta) and autolysosomes (red puncta) per cell in primary human fibroblasts expressing mCherry-EGFP-LC3B and treated with vehicle (top) or CQ (bottom) for 24 h. Scale bar: 20 µm. Data are mean ± SEM of multiple cells per condition (n = 7–29) from 6 independent cultures. Two-way ANOVA followed by Tukey's post hoc test was used as a statistical test. * P < 0.05, ** P < 0.01. # P = 0.18

1A). This biochemical profile of tau bands among tauopathies is due to the accumulation of 3R/4R-tau in FAD, 4R-tau in CBD and 3R tau in PiD [65–68]. Tau pathology was specially exacerbated in patients harboring FAD-linked *PSEN* mutations compared to other tauopathies (FAD vs. control, Tau: $P < 0.01$; Ser 396/404: $P < 0.001$; Thr 217, $P < 0.01$; Ser 202: $P < 0.01$; Thr 181, $P < 0.01$; Fig. 1A, B). When normalized to total tau, phosphorylated Ser 396/404 and Ser 202 tau species were significantly elevated in FAD and PiD, and in all tauopathies, respectively (Fig. 1B).

To examine whether accumulated tau is associated with autophagic flux failure or impaired proteasomal degradation, we examined key markers of the autophagolysosomal pathway, including the microtubule-associated autophagosome protein light chain 3 (LC3), sequestosome 1 (SQSTM1/p62), which mediates the degradation of ubiquitinated cargos, and lysosomal-associated membrane protein 2A (LAMP2A) [69] (Fig. 1C). The number of autophagosomes was assessed by measuring LC3-I conversion to LC3-II, whereas LC3-II and p62 levels were quantified to evaluate autolysosomes degradative efficiency [70]. Levels of LC3-I, LC3-II, LC3-II/I ratio and LAMP2A were unchanged in tauopathies, and only LC3 precursor (proLC3) was significantly increased in FAD ($P < 0.05$), indicating the possibility of altered autophagy flux initiation in these patients (Fig. 1D, E). By contrast, p62 was increased in FAD ($P < 0.05$), CBD ($P < 0.05$) and PiD ($P < 0.001$) cases compared to control subjects (Fig. 1D, E). Subcellular fractionation revealed that p62 was significantly increased in both soluble and insoluble hippocampal fractions of *PSEN1* carriers (fraction effect: $P < 0.0001$; group effect: $P < 0.001$; Fig. 1F). GAPDH was predominantly detected in the soluble fraction, indicating effective fractionation. This increase in p62, accompanied by unchanged LC3-II/I ratio, suggests a blockage of proteasomal degradation that can contribute to tau accumulation in *PSEN1* patients (Fig. 1C). In agreement, immunohistochemical analyses revealed a significant increase of pTau (Ser 202; $P < 0.05$) and p62 levels and its colocalization in FAD, CBD and PiD hippocampus ($P < 0.05$; Fig. 2A, B). Moreover, although LC3 levels were unchanged the percentage of pTau/LC3-positive cells was increased in the hippocampus of FAD patients ($P < 0.001$, Suppl Fig. 1A, B). Biochemical analysis of enriched fractions of autophagic vesicles revealed a significant accumulation of tau and pTau species in autophagosomes, autolysosomes and/or lysosomes in hippocampus of mutant *PSEN1* patients compared with controls ($P < 0.05$; Fig. 2C, Suppl Fig. 1C). These results suggest that although total and phosphorylated tau are degraded via autophagy, as indicated by their presence in autophagic fractions (Fig. 2C), impaired proteasomal degradation, as revealed by increased p62 and unchanged LC3-II/I ratio, may also contribute to abnormal tau accumulation in mutant *PSEN1* patients (Figs. 1D and E and 2A and B).

FAD-linked *PSEN1* mutations block autophagic flux in human primary fibroblasts

Considering the above findings in hippocampal tissue, cell-specific effects of autophagic versus proteasomal dysregulation may potentially mask the effects of *PSEN1* mutation in tau levels. For this reason, we next examined the impact of FAD-linked *PSEN1* mutations on autophagy using a cellular model lacking measurable levels of endogenous tau. Primary human skin fibroblast from healthy controls (CTRL 1 and 2) and from patients harboring *PSEN1* G206D (exon 7) and L286P (exon 8) missense mutations [61, 62] were treated with the autophagosome-lysosome fusion inhibitor chloroquine (CQ) [71]. As expected, CQ treatment increased autophagic vacuoles visualized under a bright-field microscope, and elevated p62 ($P < 0.001$), LC3-II ($P < 0.001$) and LC3-II/LC3-I ratio ($P < 0.001$; Fig. 3A–C). Fibroblasts expressing the *PSEN1* G206D and L286P mutations showed similar p62 levels in basal or CQ conditions compared to controls ($P > 0.05$, Fig. 3B, C). Interestingly, LC3-I was significantly elevated in human fibroblasts expressing FAD-linked *PSEN1* mutations in basal conditions (G206D, $P < 0.01$; L286P, $P < 0.05$) but not after CQ treatment (Fig. 3B, C). The increase of LC3-I suggests that *PSEN1* mutations potentiate autophagosomes formation and/or block autolysosomes clearance. We then evaluated autophagy flux in primary fibroblasts transiently expressing a mCherry-EGFP-LC3B reporter that allows monitoring of biogenesis of autophagosomes (mCherry+/EGFP+, yellow) and autolysosomes (mCherry+/EGFP-, red) (Fig. 3D) [72]. In basal conditions, autophagosome

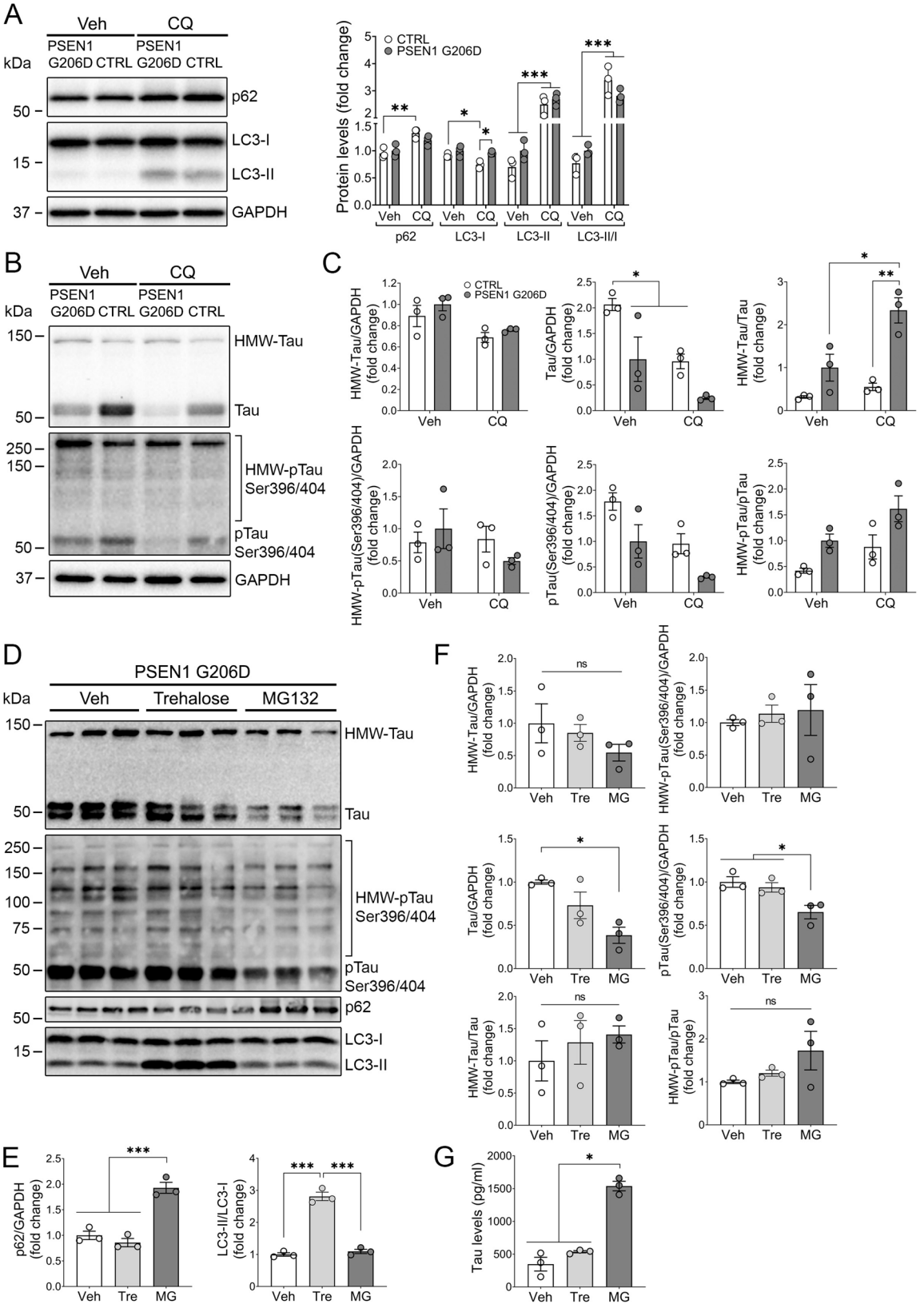

Fig. 4 (See legend on next page.)

(See figure on previous page.)

Fig. 4 Proteasome inhibition ameliorates pathological tau in human *PSEN1* G206D iPSC-derived neurons

A–C Western blot images (**A**, **B**) and quantification of p62, LC3-I, LC3-II, and LC3-II/I ratio (**A**), and total (D1M9X) and phosphorylated (p) Ser 396/404 (PHF-1) tau (**C**) in lysates of iPSC-derived neurons treated with vehicle (Veh) or 25 μM CQ for 24 h. **D-F**, Biochemical analysis of p62, LC3, and total (D1M9X) and phosphorylated (p) Ser 396/404 Tau (PHF-1) in *PSEN1* G206D neurons treated with vehicle, 100 mM trehalose (tre) or 1 μM MG132 (MG) for 24 h. Protein levels were normalized to GAPDH, LC3-I, or ~ 64–68 kDa tau, as indicated. Data represent mean ± SEM of three biological replicates per condition. **G**,Total tau in the conditioned medium of *PSEN1* G206D neurons treated with vehicle, 100 mM trehalose (Tre) or 1 μm MG132 (MG) for 24 h. Data represent mean ± SEM of three biological replicates. One- or two-way ANOVA followed by Tukey´s post hoc test was used as a statistical test. * $P < 0.05$, ** $P < 0.01$, *** $P < 0.001$, ns: not significant

number (yellow puncta) were unchanged ($P > 0.05$) and autolysosomes (red puncta) were increased in fibroblasts expressing *PSEN1* G206D (54.9 ± 7.0; $P < 0.05$) and L286P (68.1 ± 12.3; $P < 0.001$) (Fig. 3E, F). CQ induced a global increase of autophagosomes in control fibroblasts (treatment effect: $P < 0.01$), which was significantly elevated in *PSEN1* G206D fibroblasts vs. Ctrl 2 ($P < 0.05$), and mimicked the effect of *PSEN1* mutations on autolysosome accumulation ($P > 0.05$, Fig. 3E, F). The basal elevation of LC3 and autolysosomes, together with the absence of additional effects following CQ treatment, suggest that *PSEN1* mutations disrupt autophagy flux in human fibroblasts likely due to reduced lysosomal activity.

FAD-linked *PSEN1* mutations do not affect autophagy flux but enhance pathological aggregated tau in human iPSC-derived neurons

The above results promoted us to examine the levels of tau and autophagy markers in human iPSC-derived hippocampal neurons (60 DIV) from a healthy control and a patient harboring the heterozygous *PSEN1* G206D mutation [61, 62]. As expected, autophagy inhibition with CQ induced an overall increase of p62, LC3-II, and LC3-II/LC3-I ratio indicating blockade of autophagosome clearance (Treatment effect: $P < 0.001$, Fig. 4A). The absence of differences in autophagy markers between control and *PSEN1* G206D cells indicated that *PSEN1* mutation does not globally affect autophagy flux in human iPSCs-derived neurons (Fig. 4A). As shown in Fig. 4B, we found bands of ~64–68 kDa monomeric tau; and ~120–150 kDa bands of high molecular weight tau (HMW-Tau), likely corresponding to tau aggregates/oligomers [73, 74]. Surprisingly, in basal conditions, monomeric (~64–68 kDa) total and phosphorylated (Ser 396/404) tau levels were decreased in *PSEN1* G206D iPSC-derived neurons compared to control (Patient effect: $P < 0.01$), an effect that was exacerbated with CQ (Fig. 4B, C). This decrease in intracellular monomeric tau was likely due to the increase of intracellular HMW-Tau species, as suggested by higher HMW-Tau/tau ratio (Patient effect: $P < 0.01$, Fig. 4B, C). Then, we evaluated whether trehalose, which induces autophagy flux, could promote pathological tau clearance in *PSEN1* G206D iPSC-derived neurons. Trehalose induced autophagy, as indicated by increased LC3-II/I ratio ($P < 0.001$) without p62 changes (4), but did not affect monomeric or HMW-Tau levels (Fig. 4D-G), By contrast, proteasome inhibition with MG132 increased p62, reduced significantly intracellular total and phosphorylated monomeric tau levels ($P < 0.05$), without affecting HMW-Tau species, and induced tau release into the conditioned medium (Fig. 4D-G). Altogether, the FAD-linked *PSEN1 G206D* mutant does not seem to play a direct role in autophagy in iPSC-derived neurons, but it may affect directly or indirectly proteasomal-mediated tau degradation and/or release.

Loss of neuronal PS enhances phosphorylated and aggregated tau in the hippocampus of Tau transgenic mice

To investigate further the role of neuronal PS/γ-secretase on human tau pathology in vivo, we next analyzed novel PS1 cKO; Tau and PS cKO; Tau mice expressing the FTD-linked P301S tau and lacking *PS1* or both *PS*, respectively, in excitatory neurons of the postnatal forebrain [28]. Biochemical analyses showed similar total human tau levels (~4-fold change) in all Tau transgenic groups, whereas pTau at Thr 217, Ser 202 and Thr 181 were enhanced (~3-20-fold) in the hippocampus of 6 month-old PS1 cKO; Tau and/or PS cKO; Tau mice compared to WT mice (Thr 217: $P < 0.001$; Ser 202: $P < 0.01$; Thr 181: $P < 0.01$; Fig. 5A). Particularly, pTau at Ser 202 and Thr 217 were slightly increased in PS cKO; Tau mice compared to Tau and/or PS1 cKO; Tau mice ($P < 0.05$; Fig. 5A). Immunostaining confirmed increased staining of pSer 202 tau-positive neuronal somatic and projections in the hippocampus (genotype effect: CA3, $P < 0.05$; DG, $P < 0.01$), retrosplenial cortex ($P < 0.01$) and amygdala ($P < 0.01$) of PS1 cKO; Tau and PS cKO; Tau mice compared to control and/or Tau mice (Fig. 5B). Interestingly, Gallyas staining revealed abnormal conformational aggregated tau in the hippocampus and entorhinal cortex (EC) of PS cKO; Tau mice compared with control and Tau mice at 6 months (CA3: $P < 0.05$; EC: $P < 0.05$; Fig. 5C). These results indicate that total loss of *PS* function in neurons increases human tau phosphorylation and aggregation, which leads to hippocampal-dependent learning and memory deficits [28]. To understand the mechanisms leading to tau aggregation and accumulation in PS cKO; Tau mice, we analyzed markers of protein homeostasis in the hippocampus of 6 month-old mice. In agreement with our findings in human hippocampus (Figs. 1D and E and 2A and B), we found elevated levels of p62 ($P < 0.001$), the lysosomal protease CTSD ($P < 0.01$) and its precursor

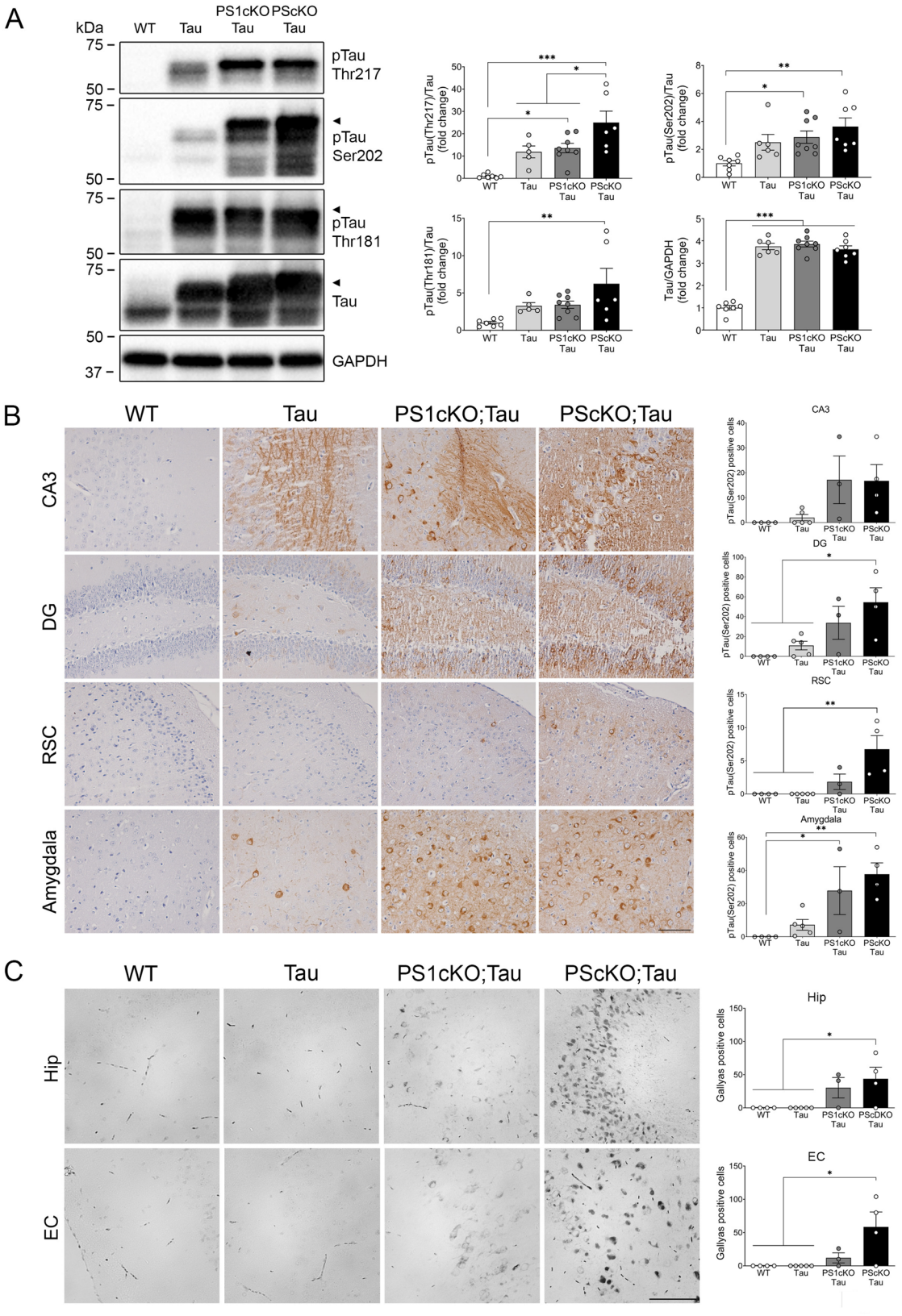

Fig. 5 (See legend on next page.)

(See figure on previous page.)

Fig. 5 Loss of neuronal PS enhances cerebral phosphorylated and aggregated human tau. **A**, Western blot analysis of pSer 202 (CP13), pThr 217, pThr 181 (AT270) and total (D1M9X) tau in the hippocampus of 6 month-old wild-type (WT) and tau transgenic mice (Tau) lacking neuronal PS1 (PS1 cKO; Tau) or both PS (PS cKO; Tau). Protein levels were normalized to GAPDH or total tau, as indicated. Values represent mean ± SEM ($n = 7$–8 mice/group). **B**, **C**, Representative immunohistochemical images and quantification of pSer202 tau (CP13) (**B**) and Gallyas-stained neurons (**C**) in coronal sections of CA3 hippocampus (Hip), dentate gyrus (DG), retrosplenial cortex RSC), entorhinal cortex (EC), and amygdala of 6 month-old non- (WT) and tau transgenic mice (Tau) lacking neuronal PS1 (PS1 cKO; Tau) or both PS (PS cKO; Tau). Scale bar: 100 µm. Values represent mean of pSer202 Tau or Gallyas-positive cells/section ± SEM ($n = 3$ slices per mice, 4 mice/group). Statistical analysis was determined by one-way ANOVA followed by Tukey's (**A**, **C**) or Bonferroni's (**B**) post hoc tests. *$P < 0.05$, **$P < 0.01$, ***$P < 0.001$

proCTSD ($P < 0.001$) but unaltered LC3-II/I ratio in hippocampal lysates of PS cKO; Tau mice at 6 months (Fig. 6A, B). This suggests blockade of proteasomal degradation and potentially a compensatory mechanism to clear aggregated tau via lysosomal degradation. Biochemical analyses showed significant increases of active pAkt (Ser 473,Thr 308) and its downstream phosphorylated substrates GSK3β (Ser 9; $P < 0.05$) and proline-rich Akt substrate (PRAS40, Thr 246; $P < 0.001$) in hippocampal lysates of PS cKO; Tau mice (Fig. 6A–D). Analysis of the mTOR signaling pathway – a key regulator of autophagy initiation – corroborated our hypothesis of unaltered autophagy flux in PS cKO; Tau mice, as no significant changes compared to control group were observed in phosphorylated mTOR (Ser 2448) or its downstream effectors ULK1 (Ser 757), p70S6K (Thr 389) and S6 (Ser 235/236) (Fig. 6C–E). Together, these findings suggest that complete loss of PS function affects key proteasomal and lysosomal molecules essential for tau degradation in neurons.

PS regulates proteasome-dependent tau secretion in human tau-expressing neurons

To further investigate the link between PS-dependent tau pathology and proteasome/autophagy pathways, we analyzed primary neurons obtained from human tau (Tau+) transgenic embryos harboring floxed *PS1*;*PS2*$^{+/+}$ or *PS1*;*PS2*$^{-/-}$ alleles. Neurons were transduced with lentiviral vectors containing inactive (no recombination) or active Cre-recombinase for efficient conditional silencing of PS1 (PS1 cKO; Tau) or both PS (PS cKO; Tau) ($P < 0.001$, Fig. 7A). Primary cortical neurons were treated with CQ, MG132 (MG), or the combination CQ/MG132 to inhibit autophagy and/or proteasomal degradation, as indicated by increased p62 and LC3-II/LC3-I ratio, or by accumulation of p62 and ubiquitinated proteins, respectively (treatment effect: $P < 0.01$-0.0001; Fig. 7A, C). 24 h-treatment with CQ or MG was not cytotoxic (~ 90–100% cell viability), whereas their combination reduced slightly neuron viability (~ 78% cell viability; $P < 0.001$).

Consistently with our previous results in iPSC-derived *PSEN1* G206D neurons (Fig. 4), blocking proteasome (MG) alone or together with autophagy (CQ + MG) reduced intracellular phosphorylated (Ser202 and Ser396/404) and/or total tau levels (treatment effect: $P < 0.001$; Fig. 7A, B). Furthermore, MG and CQ/MG increased levels of extracellular human tau in Tau and PS1 cKO; Tau neurons ($P < 0.001$), an effect significantly reduced in PS cKO; Tau neurons ($P < 0.05$; Fig. 7D). Correlation analysis of intracellular versus released extracellular human tau showed that MG-treated samples clustered together but separately from vehicle and CQ samples (Fig. 7E). Notably, intraneuronal tau was negatively correlated with extracellular tau independently of the genotype, and this correlation was less pronounced in PS cKO; Tau neurons (Fig. 7E). These findings suggest that proteasomal inhibition reduces intracellular tau levels by promoting its extracellular release through a mechanism that depends partially on PS.

Discussion

The accumulation of hyperphosphorylated tau aggregates is a common pathological hallmark of tauopathies, including those caused by autosomal dominant *PSEN1* mutations, irrespective of whether such mutations enhance or not cerebral Aβ. The precise mechanisms by which *PSEN1* mutations lead to tau accumulation, aggregation, and secretion remain incompletely understood. The present investigation elucidated key aspects of these pathways while providing insights for the identification of novel biomarkers and therapeutic targets for dementia. Our study revealed increased pathological pTau associated with elevated ubiquitin-binding factor p62 in the hippocampus of patients with FAD-linked *PSEN1* mutations and neuronal *PS*-deficient tau mice, which suggests that loss of PS function disrupts tau proteasomal degradation. Notably, pharmacological proteasome inhibition reduced intracellular total and pTau levels while increasing extracellular tau release in human mutant *PSEN1* iPSC- and *PS* deficient tau-derived neurons. These results demonstrate that PS regulates proteasome-mediated tau elimination in neurons, and that FAD-linked *PSEN1* mutations cause tau pathology by disrupting the proteasome and autophagy/lysosomal pathways (Fig. 7F).

Accumulation of autophagic vesicles and autolysosomes in dystrophic neurites with neurofibrillary pathology are detected in sporadic and APP-linked FAD, CBD, and PSP [31–33], suggesting disruption of autophagy-mediated tau clearance. In agreement, we found that phosphorylated aggregated tau was present in autophagic vesicles from the hippocampus of FAD patients,

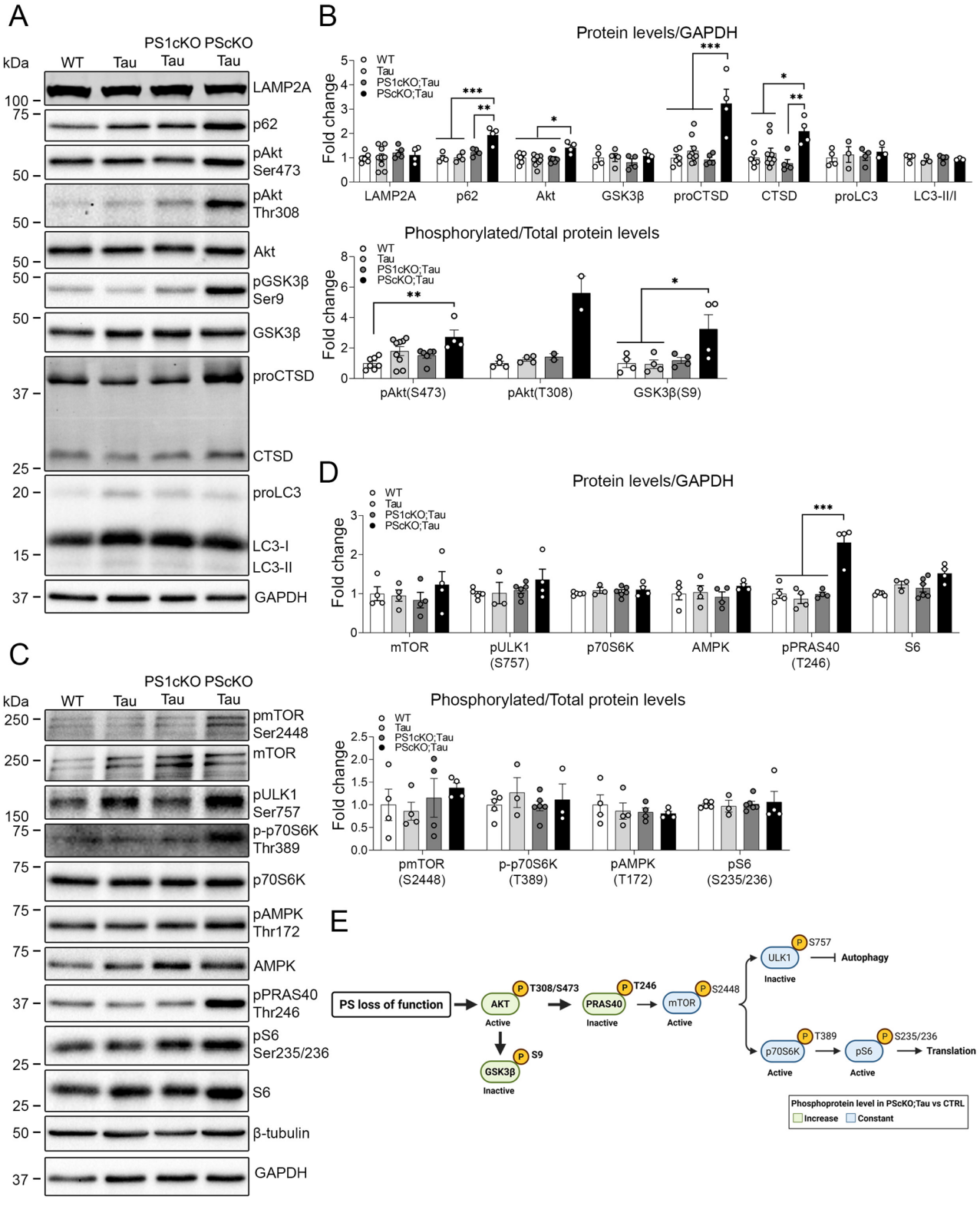

Fig. 6 (See legend on next page.)

(See figure on previous page.)

Fig. 6 Loss of neuronal PS enhances p62 and Akt phosphorylation. **A**, **B** Biochemical analysis and quantification of phosphorylated and/or total LAMP2A, p62, Akt, GSK3β, CTSD, and in hippocampal lysates of 6 month-old WT, Tau, PS1 cKO; Tau, PS cKO; Tau transgenic mice. Proteins were normalized to GAPDH and phosphorylated proteins to their corresponding total proteins. **C**, **D**, Biochemical analysis and quantification of phosphorylated and/or total mTOR, ULK1, p70S6K, AMPK, PRAS40 and S6 in hippocampal lysates of 6 month-old WT, Tau, PS1 cKO; Tau, PS cKO; Tau transgenic mice. Phosphorylated proteins were normalized to their corresponding total proteins (except for pULK1 and pPRAS40), and total proteins were normalized to GAPDH except for pPRAS40 that was normalized to β-tubulin. **E**, Scheme showing the presenilin-dependent molecular pathways regulating Akt/GSK3β and mTORC pathways in neurons. Data represent mean ± SEM ($n = 3$–9 mice/group). Statistical analysis was determined by one-way ANOVA followed by Tukey's post hoc tests. $^{*}P < 0.05$, $^{**}P < 0.01$, $^{***}P < 0.001$

indicating that tau aggregates are degraded via autophagy. In human fibroblasts harbouring *PSEN1* mutations there was a deficient clearance of autolysosomes, resembling the effect of CQ treatment. These observations are consistent with previous results showing that mutations in *PSEN1* impair autophagy flux through defective lysosomal acidification, fusion, or enzymatic activity [49–76]. Phosphorylated mTOR accumulates in AD brains and is associated with tau hyperphosphorylation [77]. In PS-deficient fibroblasts and AD iPSC-derived neurons, active mTOR remains tethered to the lysosomal membrane, impairing autophagy by inhibiting TFEB-dependent transcription of autophagy and lysosomal genes [49, 56]. By contrast, reduced phosphorylated mTOR is associated with enhanced autophagy initiation but impaired autophagosomes clearance in PS-deficient fibroblasts [55]. We did not find any effect of neuronal PS deficiency on mTOR signalling and phosphorylation of its downstream effector ULK1 at Ser 757, responsible for autophagy initiation, although ULK1 phosphorylation at Ser 405/415 by GSK3β can also promote autophagy initiation [78]. Interestingly, Akt-induced GSK3β inactivation could contribute to altered autophagy in PS cKO; Tau mice, but further analysis of GSK3β/ULK1 signaling is required to confirm its involvement in autophagy-mediated tau degradation.

The minimal changes in autophagy markers along with unchanged LC3-II/I ratio detected in hippocampus of patients harboring *PSEN1* mutations and in our mouse models, prompted us to investigate alternative tau clearance pathways. A common feature identified in the hippocampus of *PSEN1* carriers and PS cKO; Tau mice was both the accumulation of pathological tau and p62, which is as a key adaptor protein that delivers ubiquitinated cargo to autophagy and functionally links the UPS and autophagy pathways [69]. Our results suggested that PS dysfunction caused by autosomal FAD-linked mutations or genetic loss alters proteasomal tau degradation, a result consistent with the established role of the autophagy/lysosome and proteasome pathways on tau degradation [47]. Indeed, significant efforts have been focused towards the development of therapeutic strategies aimed at enhancing tau degradation via the proteasome [47]. Considering that the molecular mechanisms linking PS and proteasome degradation are largely unknown, our finding that Akt is activated in the hippocampus of PS cKO; Tau mice is highly relevant. Besides being an upstream regulator of mTOR, Akt inhibits autophagy-mediated Aβ clearance [43] and mediates the activation of USP14 [79], a deubiquitinating enzyme that inhibits the UPS and blocks protein degradation. Interestingly, tau deubiquitination by USP10 increases tau phosphorylation, aggregation and accumulation, whereas inhibition of USP14 potentiates proteasomal tau clearance, supporting the importance of UPS in tau degradation [80, 81]. Together, we propose that PS loss of function in neurons leads to increased Akt activity, UPS inhibition and tau accumulation (Fig. 7F). Surprisingly, proteasome inhibition in cultured neurons reduced intraneuronal tau and enhanced its secretion, a process partially dependent on PS. Whether tau is released via extracellular vesicles (EVs) or freely into the extracellular medium in these conditions merits further investigation. Interestingly, EVs isolated from *PSEN1* iPSC-neurons induce tau hyperphosphorylation in vivo [82], an effect explained by the alteration of the EV proteome [83]. Altogether, these findings highlight the critical role of PS and UPS in the degradation and secretion of tau in neurons, a mechanism critical for its cell-to-cell propagation.

In summary, the crosstalk between autophagy and the proteasome may influence the progression of tau pathology in dementias. Autophagy and proteasomal degradation are highly interconnected proteostatic pathways, wherein dysregulation of one system can elicit compensatory upregulation of the other [69]. The elevated proLC3 and LC3 levels in the hippocampus and/or fibroblasts of FAD patients suggest an enhancement of autophagy initiation, potentially as a compensatory response for defective proteasomal degradation. The increase of proCTSD and CTSD in the hippocampus of PS cKO; Tau mice may reflect a compensatory mechanism to enhance lysosomal degradative activity to restore neuronal proteostasis. CTSD is implicated in the processing of APP and tau, and in the clearance of Aβ aggregates [84, 85], but increased CTSD levels can also lead to cell death [86]. In addition, several genetic risk factors associated with AD, including *APOE4*, *BIN1*, *PICALM*, *PSEN*, and *SORL1*, are known to regulate the endosomal-lysosomal pathway. This convergence suggests that the effects of inherited *PSEN1* mutations on neuronal autophagy and lysosomal function may be modulated by these AD risk genes. Consistent with this notion, recent single-nucleus transcriptomics

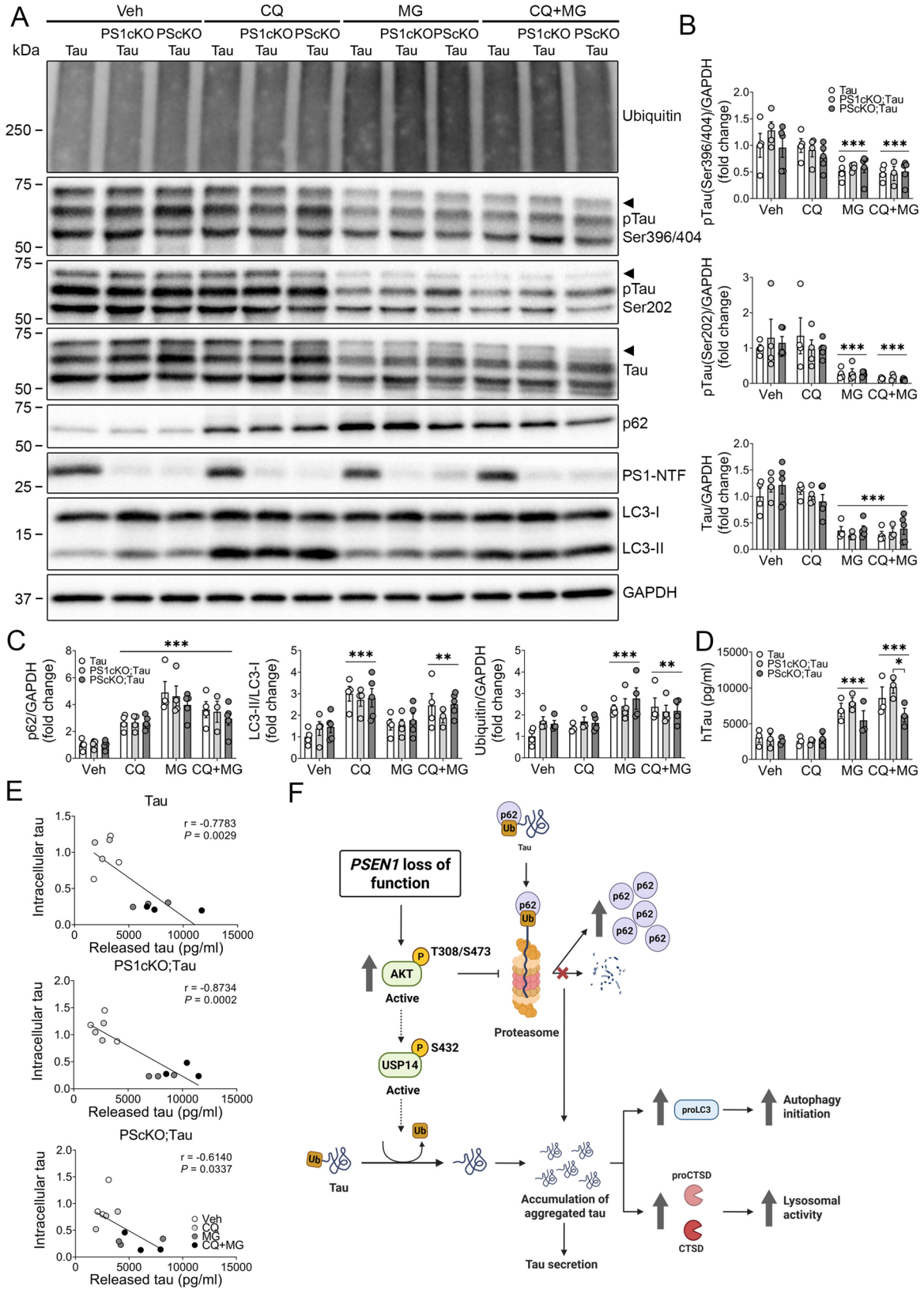

Fig. 7 (See legend on next page.)

(See figure on previous page.)

Fig. 7 PS regulates tau release induced by proteasome inhibition in primary cortical neurons. **A**–**C**, Western blot images and quantitative analyses of phosphorylated (p) tau Ser 396/404 (PHF-1) and Ser 202 (CP13), total tau (D1M9X), PS1 NTF, and autophagy and ubiquitin markers in protein lysates of primary cortical neurons (12 DIV) treated with vehicle (Veh), chloroquine (CQ) and/or MG132 (MG) for 24 h. Protein levels were normalized to GAPDH, and values represent mean ± SEM (n = 4–5 embryos/group of 3 independent cultures). **D**, Secreted human (h) tau levels in the cell medium of primary cortical neurons (12 DIV) treated with Veh, CQ and/or MG132 for 24 h measured by ELISA. Values represent mean ± SEM (n = 3 embryos/group in 2 inde¬pendent cultures). In **A**–**D**, statistical analysis was determined by two-way ANOVA followed by Tukey's post hoc tests. *P < 0.05, **P < 0.01, ***P < 0.001 vs. Vehicle. **E**, Correlation analyses of intracellular and released hTau levels in primary cortical neurons overexpressing human tau and lacking PS1 (PS1 cKO; Tau) or both PS (PS cKO; Tau), and treated with Veh, CQ and/or MG132 for 24 h. Data was analyzed using two-tailed Pearson's (r) correlation coefficient. **F**, Hypothetical model of Presenilin-dependent molecular pathways regulating proteasome-mediated tau degradation in neurons. Loss of PSEN1 function activates Akt (pAkt Thr308/Ser473) leading to UPS inhibition, as evidenced by elevated p62, and potentially activates USP14 (dashed lines), which could lead to tau deubiquitination and accumulation. Blockade of tau degradation via proteasome contributes to tau secretion and disease progression. As a compensatory response to UPS dysfunction, proLC3 and proCTSD and CTSD are increased, indicating enhanced autophagy initiation and lysosomal activity, respectively. USP14: ubiquitin-specific protease 14; Ub: ubiquitin; proCTSD: pro-cathepsin D; CTSD: cathepsin D

has demonstrated significant enrichment of autophagy- and chaperone-related genes in astrocytes and neurons from the frontal cortex of *PSEN1* E280A AD patients [87].Future investigations should elucidate the molecular mechanisms by which presenilin orchestrates proteostasis-related gene networks and how dysregulation of these pathways influences the progression and clearance of tau pathology.

Abbreviations

AD	Alzheimer's disease
Akt/PKB	Protein kinase B
AL	Autolysosome
AMPK	AMP-activated kinase
Aph	Autophagosome
APP	Amyloid precursor protein
Aβ	β-Amyloid
CaMKIIα	Ca^{2+}/Calmodulin-dependent protein kinase II subunit alpha
CBD	Corticobasal degeneration
CBP	CREB-binding protein
cKO	Conditional knockout
CQ	Chloroquine
CREB	CAMP response element binding protein
CTRL	Control
CTSD	Cathepsin D
DG	Dentate gyrus
DIV	Days in vitro
EC	Entorhinal cortex
EF1α	Elongation factor 1-alpha
EGFP	Enhanced green fluorescent protein
ELISA	Enzyme-linked immunosorbent assay
FAD	Familial Alzheimer's disease
FTD	Frontotemporal dementia
GAPDH	Glyceraldehyde-3-phosphate dehydrogenase
GSK3β	Glycogen synthase kinase-3 β
Hip	Hippocampus
LAMP2	Lysosomal-associated protein 2A
LC3	Microtubule-associated protein light chain 3
Lys	Lysosomes
MAPT	Microtubule-associated protein tau
mTOR	Mammalian target of rapamycin
NFTs	Neurofibrillary tangles
PiD	Pick's disease
PRAS40	Proline-rich Akt substrate 40
PrP	Prion protein promoter
PS/PSEN	Presenilin
PSP	Progressive supranuclear palsy
pTau	Phosphorylated tau
RSC	Retrosplenial cortex
SEM	Standard error of the mean
SQSTM1/p62	Sequestosome 1
ULK1	Unc-51-like kinase 1
Veh	Vehicle
WT	Wild type

Supplementary Information

The online version contains supplementary material available at https://doi.org/10.1186/s40478-026-02270-6.

Supplementary Fig. 1. Somatic phosphorylated tau colocalizes with the autophagy marker LC3 in the hippocampus of tauopathy patients. **A** Representative immunofluorescence images of hippocampal sections from a healthy control (CTRL), and FAD, CBD and PiD patients stained for pSer 202 tau (CP13, green) and LC3 (red). Images correspond to CTRL 12, FAD 7, CBD 5 and PiD 6. Scale bar: 20 µm. **B**, Quantitative analysis of total LC3 intensity per area. Data represent mean ± SEM of multiple individuals ($n = 6–7$) per group. Statistical analysis was determined by one-way ANOVA followed by Tukey's post hoc tests. *** $P < 0.001$. **C**, Biochemical analysis of autophagic and lysosome markers in purified autophagic and lysosomal fractions from control hippocampus. Representative images corresponding to CTRL 13. L: total lysate; Aph: autophagosomes; AL: autolysosomes; Lys: lysosomes. CTSD: cathepsin D.

Supplementary Material 2

Acknowledgements

We are indebted to the Biobanc-Hospital Clinic-FRCB-IDIBAPS for samples and data procurement, and the professionals of Servei d'Estabulari-UAB, Cell Culture, Histology and Microscope facilities at Institut de Neurociències-UAB. We thank José R. Bayascas for technical antibody advice and sharing reagents, Meritxell Lara for technical microscopy support, and Francisco J. Fernández Acosta for helping with the cell culture of iPSC-derived neurons.

Author contributions

AdSB, CMSF and CAS designed and coordinated the study. AdSB and CMSF designed and performed the biochemical, pathological and immunofluorescence analyses in human and mouse brains and cultured neurons. CV performed biochemical analysis. LMP provided and reviewed the neuropathological analyses of human samples. RSV provided clinical and genetic information of human AD samples. RV and CV generated, characterized and performed experiments of the human fibroblasts and iPSC-derived neurons. AdSB, CMSF, RV, JRA AD, CV and CAS discussed and interpreted the data. AdSB, CMSF and CAS wrote the manuscript with input of all authors. All authors read and approved the final manuscript.

Funding

This work was supported by research grants funded by Ministerio de Ciencia, Innovación y Universidades from Spain MICIU/AEI/10.13039/501100011033 with FEDER and "European UnionNextGenerationEU"/PRTR" funds (PID2019-106615RB-I00, PID2022-137668OB-I00 and PDC2022-133831-I00 to CAS, and PID2019-109059RB-I00 and PID2022-137076OB-I00 to CV), Instituto de Salud Carlos III (CIBERNED CB06/05/0042 and CB06/05/0065 to JRA and CV; CIBERNED Traslational collaborative project PI2021/04), Generalitat de Catalunya (2021 SGR00142), and BrightFocus Foundation (A2022047S). AdSB (FI_B00858), CMSF (FI_B00326) and CV (Joan Oró Fellowship 2023FI_1_01104) were supported by FI predoctoral fellowships from AGAUR/Generalitat de Catalunya.

Data availability
Data generated or analysed during this study are included in this published article [and its supplementary information files]. Materials described in the manuscript are available upon request.

Declarations

Ethics approval and consent to participate
The use of human samples was approved by the Human Ethical Committee of Hospital Clinic-IDIBAPS and Universitat Autònoma de Barcelona (CEEAH 3724). All patients' data and samples were coded and handled according to national guidelines to protect patients' identities. Animal procedures were conducted according to the Animal and Human Ethical Committee of the Universitat Autònoma de Barcelona approved by Generalitat de Catalunya (CEEAH 2895/DMAH 10571) following European Union guidelines and regulations (2010/63, 2016/679).

Consent for publication
Not applicable.

Competing interests
The authors declare no competing interests.

Author details
[1]Institut de Neurociències, Departament de Bioquímica i Biologia Molecular, Facultat de Medicina, Universitat Autònoma de Barcelona, 08193 Bellaterra, Barcelona, Spain
[2]Centro de Investigación Biomédica en Red Enfermedades Neurodegenerativas (CIBERNED), Instituto de Salud Carlos III (ISCIII), 28029 Madrid, Spain
[3]Instituto Cajal, Consejo Superior de Investigaciones Científicas (CSIC), 28002 Madrid, Spain
[4]Centro de Neurociencias Cajal, CSIC, Campus de Alcalá de Henares, 28805 Madrid, Spain
[5]Alzheimer's Disease and Other Cognitive Disorders Unit, Neurology Department, Hospital Clínic, Fundació de Recerca Clínic Barcelona-Institut d'Investigacions Biomèdiques August Pi i Sunyer (FRCB-IDIBAPS), Institute of Neurosciences, Universitat de Barcelona, 08036 Barcelona, Spain
[6]Neurological Tissue Bank, Biobanc-Hospital Clínic, FRCB/IDIBAPS, 08036 Barcelona, Spain
[7]Hospital Universitari Parc Taulí, Institut d'Investigació i Innovació Parc Taulí (I3PT-CERCA), Universitat Autònoma de Barcelona, 08208 Sabadell, Spain
[8]Present address: Sir William Dunn School of Pathology, University of Oxford, Oxford OX1 3RE, UK
[9]Present address: Department of Neurology, Jungers Center for Neurosciences Research, Oregon Health Science University, Portland, OR 97239, USA

Received: 29 October 2025 / Accepted: 21 February 2026
Published online: 20 March 2026

References

1. Ittner LM, Gotz J (2011) Amyloid-β and tau–a toxic pas de deux in Alzheimer's disease. Nat Rev Neurosci 12:65–72. https://doi.org/10.1038/nrn2967
2. Spires-Jones TL, Hyman BT (2014) The intersection of amyloid-β and tau at synapses in Alzheimer's disease. Neuron 82:756–771. https://doi.org/10.1016/j.neuron.2014.05.004
3. Arriagada PV, Growdon JH, Hedley-Whyte ET, Hyman BT (1992) Neurofibrillary tangles but not senile plaques parallel duration and severity of Alzheimer's disease. Neurology 42:631–639
4. Gomez-Isla T, Hollister R, West H, Mui S, Growdon J, Peterson R, Parisi J, Hyman B (1997) Neuronal loss correlates with but exceeds neurofibrillary tangles in Alzheimer's disease. Ann Neurol 41:17–24
5. Ashton NJ, Janelidze S, Mattsson-Carlgren N, Binette AP, Strandberg O, Brum WS, Karikari TK, Gonzalez-Ortiz F, Di Molfetta G, Meda FJ al (2022) Differential roles of Aβ42/40, p-tau231 and p-tau217 for Alzheimer's trial selection and disease monitoring. Nat Med 28:2555–2562. https://doi.org/10.1038/s41591-022-02074-w
6. Frank B, Ally M, Brekke B, Zetterberg H, Blennow K, Sugarman MA, Ashton NJ, Karikari TK, Tripodis Y, Martin Bet al et al (2022) Plasma p-tau181 shows stronger network association to Alzheimer's disease dementia than neurofilament light and total tau. Alzheimers Dement 18:1523–1536. https://doi.org/10.1002/alz.12508
7. Janelidze S, Mattsson N, Palmqvist S, Smith R, Beach TG, Serrano GE, Chai X, Proctor NK, Eichenlaub U, Zetterberg Het al et al (2020) Plasma P-tau181 in Alzheimer's disease: relationship to other biomarkers, differential diagnosis, neuropathology and longitudinal progression to Alzheimer's dementia. Nat Med 26:379–386. https://doi.org/10.1038/s41591-020-0755-1
8. Simrén J, Leuzy A, Karikari TK, Hye A, Benedet AL, Lantero-Rodriguez J, Mattsson-Carlgren N, Scholl M, Mecocci P, Vellas Bet al et al (2021) The diagnostic and prognostic capabilities of plasma biomarkers in Alzheimer's disease. Alzheimers Dement 17:1145–1156. https://doi.org/10.1002/alz.12283
9. De Strooper B, Iwatsubo T, Wolfe MS (2012) Presenilins and γ-secretase: structure, function, and role in Alzheimer's disease. Cold Spring Harb Perspect Med 2:a006304. https://doi.org/10.1101/cshperspect.a006304
10. Gomez-Isla T, Growdon WB, McNamara MJ, Nochlin D, Bird TD, Arango JC, Lopera F, Kosik KS, Lantos PL, Cairns NJ et al (1999) The impact of different presenilin 1 and presenilin 2 mutations on amyloid deposition, neurofibrillary changes and neuronal loss in the familial Alzheimer's disease brain: evidence for other phenotype-modifying factors. Brain 122(Pt9):1709–1719
11. Petit D, Fernandez SG, Zoltowska KM, Enzlein T, Ryan NS, O'Connor A, Szaruga M, Hill E, Vandenberghe R, Fox NCet al et al (2022) Aβ profiles generated by Alzheimer's disease causing PSEN1 variants determine the pathogenicity of the mutation and predict age at disease onset. Mol Psychiatry 27:2821–2832. https://doi.org/10.1038/s41380-022-01518-6
12. Sudo S, Shiozawa M, Cairns NJ, Wada Y (2005) Aberrant accentuation of neurofibrillary degeneration in the hippocampus of Alzheimer's disease with amyloid precursor protein 717 and presenilin-1 gene mutations. J Neurol Sci 234:55–65 Doi S0022-510X(05)00112-7 [pii]. https://doi.org/10.1016/j.jns.2005.03.043
13. Woodhouse A, Shepherd CE, Sokolova A, Carroll VL, King AE, Halliday GM, Dickson TC, Vickers JC (2009) Cytoskeletal alterations differentiate presenilin-1 and sporadic Alzheimer's disease. Acta Neuropathol 117:19–29. https://doi.org/10.1007/s00401-008-0458-z
14. Ittner LM, Ke YD, Delerue F, Bi M, Gladbach A, van Eersel J, Wolfing H, Chieng BC, Christie MJ, Napier IA (2010) Dendritic function of tau mediates amyloid-β toxicity in Alzheimer's disease mouse models. Cell 142:387–397. https://doi.org/10.1016/j.cell.2010.06.036
15. Pickett EK, Herrmann AG, McQueen J, Abt K, Dando O, Tulloch J, Jain P, Dunnett S, Sohrabi S, Fjeldstad MP (2019) al Amyloid-β and tau cooperate to cause reversible behavioral and transcriptional deficits in a model of Alzheimer's sisease. Cell Rep 29:3592–3604 e3595. https://doi.org/10.1016/j.celrep.2019.11.044
16. Roberson ED, Scearce-Levie K, Palop JJ, Yan F, Cheng IH, Wu T, Gerstein H, Yu GQ, Mucke L (2007) Reducing endogenous tau ameliorates amyloid β-induced deficits in an Alzheimer's disease mouse model. Science 316:750–754. https://doi.org/10.1126/science.1141736
17. DeVos SL, Corjuc BT, Commins C, Dujardin S, Bannon RN, Corjuc D, Moore BD, Bennett RE, Jorfi M, Gonzales JA al (2018) Tau reduction in the presence of amyloid-β prevents tau pathology and neuronal death in vivo. Brain 141:2194–2212. https://doi.org/10.1093/brain/awy117
18. Goedert M, Eisenberg DS, Crowther RA (2017) Propagation of tau aggregates and neurodegeneration. Annu Rev Neurosci 40:189–210. https://doi.org/10.1146/annurev-neuro-072116-031153
19. Bernardi L, Tomaino C, Anfossi M, Gallo M, Geracitano S, Costanzo A, Colao R, Puccio G, Frangipane F, Curcio SA al (2009) Novel PSEN1 and PGRN mutations in early-onset familial frontotemporal dementia. Neurobiol Aging 30:1825–1833. https://doi.org/10.1016/j.neurobiolaging.2008.01.005
20. Dermaut B, Kumar-Singh S, Engelborghs S, Theuns J, Rademakers R, Saerens J, Pickut BA, Peeters K, Van Den Broeck M, Vennekens K (2004) A novel presenilin 1 mutation associated with Pick's disease but not β-amyloid plaques. Ann Neurol 55:617–626
21. Larner AJ, Doran M (2006) Clinical phenotypic heterogeneity of Alzheimer's disease associated with mutations of the presenilin-1 gene. J Neurol 253:139–158. https://doi.org/10.1007/s00415-005-0019-5
22. Raux G, Gantier R, Thomas-Anterion C, Boulliat J, Verpillat P, Hannequin D, Brice A, Frebourg T, Campion D (2000) Dementia with prominent frontotemporal features associated with L113P presenilin 1 mutation. Neurology 55:1577–1578

23. Dewachter I, Ris L, Croes S, Borghgraef P, Devijver H, Voets T, Nilius B, Godaux E, Van Leuven F (2008) Modulation of synaptic plasticity and Tau phosphorylation by wild-type and mutant presenilin1. Neurobiol Aging 29:639–652. https://doi.org/10.1016/j.neurobiolaging.2006.11.019
24. Ochalek A, Mihalik B, Avci HX, Chandrasekaran A, Teglasi A, Bock I, Giudice ML, Tancos Z, Molnar K, Laszlo L et al (2017) Neurons derived from sporadic Alzheimer's disease iPSCs reveal elevated tau hyperphosphorylation, increased amyloid levels, and GSK3B activation. Alzheimers Res Ther 9:90. https://doi.org/10.1186/s13195-017-0317-z
25. Xia D, Watanabe H, Wu B, Lee SH, Li Y, Tsvetkov E, Bolshakov VY, Shen J, Kelleher RJ (2015) Presenilin-1 knockin mice reveal loss-of-function mechanism for familial Alzheimer's disease. Neuron 85:967–981. https://doi.org/10.1016/j.neuron.2015.02.010
26. Lleó A, Saura CA (2011) γ-secretase substrates and their implications for drug development in Alzheimer's disease. Curr Top Med Chem 11:1513–1527 Doi BSP/CTMC/E-Pub/-000130-11-16 [pii]
27. Saura CA, Choi SY, Beglopoulos V, Malkani S, Zhang D, Shankaranarayana Rao BS, Chattarji S, Kelleher RJ, Kandel ER, Duff Ket al et al (2004) Loss of presenilin function causes impairments of memory and synaptic plasticity followed by age-dependent neurodegeneration. Neuron 42:23–36https://doi.org/10.1016/S0896-6273(04)00182-5
28. Soto-Faguas CM, Sanchez-Molina P, Saura CA (2021) Loss of presenilin function enhances tau phosphorylation and aggregation in mice. Acta Neuropathol Commun 9:162. https://doi.org/10.1186/s40478-021-01259-7
29. Watanabe H, Iqbal M, Zheng J, Wines-Samuelson M, Shen J (2014) Partial loss of presenilin impairs age-dependent neuronal survival in the cerebral cortex. J Neurosci 34:15912–15922. https://doi.org/10.1523/JNEUROSCI.3261-14.2014
30. Menzies FM, Fleming A, Caricasole A, Bento CF, Andrews SP, Ashkenazi A, Fullgrabe J, Jackson A, Jimenez Sanchez M, Karabiyik C et al (2017) Autophagy and neurodegeneration: pathogenic mechanisms and therapeutic opportunities. Neuron 93:1015–1034. https://doi.org/10.1016/j.neuron.2017.01.022
31. Boland B, Kumar A, Lee S, Platt FM, Wegiel J, Yu WH, Nixon RA (2008) Autophagy induction and autophagosome clearance in neurons: relationship to autophagic pathology in Alzheimer's disease. J Neurosci 28:6926–6937. https://doi.org/10.1523/JNEUROSCI.0800-08.2008
32. Nixon RA, Wegiel J, Kumar A, Yu WH, Peterhoff C, Cataldo A, Cuervo AM (2005) Extensive involvement of autophagy in Alzheimer disease: an immunoelectron microscopy study. J Neuropathol Exp Neurol 64:113–122. https://doi.org/10.1093/jnen/64.2.113
33. Piras A, Collin L, Gruninger F, Graff C, Ronnback A (2016) Autophagic and lysosomal defects in human tauopathies: analysis of post-mortem brain from patients with familial Alzheimer disease, corticobasal degeneration and progressive supranuclear palsy. Acta Neuropathol Commun 4:22. https://doi.org/10.1186/s40478-016-0292-9
34. Caballero B, Bourdenx M, Luengo E, Diaz A, Sohn PD, Chen X, Wang C, Juste YR, Wegmann S, Patel Bet al et al (2021) Acetylated tau inhibits chaperone-mediated autophagy and promotes tau pathology propagation in mice. Nat Commun 12:2238. https://doi.org/10.1038/s41467-021-22501-9
35. Caballero B, Wang Y, Diaz A, Tasset I, Juste YR, Stiller B, Mandelkow EM, Mandelkow E, Cuervo AM (2018) Interplay of pathogenic forms of human tau with different autophagic pathways. Aging Cell 17:e12692. https://doi.org/10.1111/acel.12692
36. Kruger U, Wang Y, Kumar S, Mandelkow EM (2012) Autophagic degradation of tau in primary neurons and its enhancement by trehalose. Neurobiol Aging 33:2291–2305. https://doi.org/10.1016/j.neurobiolaging.2011.11.009
37. Bourdenx M, Martin-Segura A, Scrivo A, Rodriguez-Navarro JA, Kaushik S, Tasset I, Diaz A, Storm NJ, Xin Q, Juste YR (2021) al Chaperone-mediated autophagy prevents collapse of the neuronal metastable proteome. Cell 184:2696–2714 e2625. https://doi.org/10.1016/j.cell.2021.03.048
38. Caccamo A, Magri A, Medina DX, Wisely EV, Lopez-Aranda MF, Silva AJ, Oddo S (2013) mTOR regulates tau phosphorylation and degradation: implications for Alzheimer's disease and other tauopathies. Aging Cell 12:370–380. https://doi.org/10.1111/acel.12057
39. Ozcelik S, Fraser G, Castets P, Schaeffer V, Skachokova Z, Breu K, Clavaguera F, Sinnreich M, Kappos L, Goedert Met al et al (2013) Rapamycin attenuates the progression of tau pathology in P301S tau transgenic mice. PLoS ONE 8:e62459. https://doi.org/10.1371/journal.pone.0062459
40. Schaeffer V, Lavenir I, Ozcelik S, Tolnay M, Winkler DT, Goedert M (2012) Stimulation of autophagy reduces neurodegeneration in a mouse model of human tauopathy. Brain 135:2169–2177. https://doi.org/10.1093/brain/aws143
41. Silva MC, Nandi GA, Tentarelli S, Gurrell IK, Jamier T, Lucente D, Dickerson BC, Brown DG, Brandon NJ, Haggarty SJ (2020) Prolonged tau clearance and stress vulnerability rescue by pharmacological activation of autophagy in tauopathy neurons. Nat Commun 11:3258. https://doi.org/10.1038/s41467-020-16984-1
42. Wani A, Al Rihani SB, Sharma A, Weadick B, Govindarajan R, Khan SU, Sharma PR, Dogra A, Nandi U, Reddy CN al (2021) Crocetin promotes clearance of amyloid-beta by inducing autophagy via the STK11/LKB1-mediated AMPK pathway. Autophagy 17:3813–3832. https://doi.org/10.1080/15548627.2021.1872187
43. Wani A, Gupta M, Ahmad M, Shah AM, Ahsan AU, Qazi PH, Malik F, Singh G, Sharma PR, Kaddoumi Aet al et al (2019) Alborixin clears amyloid-beta by inducing autophagy through PTEN-mediated inhibition of the AKT pathway. Autophagy 15:1810–1828. https://doi.org/10.1080/15548627.2019.1596476
44. Akwa Y, Gondard E, Mann A, Capetillo-Zarate E, Alberdi E, Matute C, Marty S, Vaccari T, Lozano AM, Baulieu EE et al (2018) Synaptic activity protects against AD and FTD-like pathology via autophagic-lysosomal degradation. Mol Psychiatry 23:1530–1540. https://doi.org/10.1038/mp.2017.142
45. 63 Pooler AM, Phillips EC, Lau DH, Noble W, Hanger DP (2013) Physiological release of endogenous tau is stimulated by neuronal activity. EMBO Rep 14:389–394. https://doi.org/10.1038/embor.2013.15
46. Yamada K, Holth JK, Liao F, Stewart FR, Mahan TE, Jiang H, Cirrito JR, Patel TK, Hochgrafe K, Mandelkow EMet al et al (2014) Neuronal activity regulates extracellular tau in vivo. J Exp Med 211:387–393. https://doi.org/10.1084/jem.20131685
47. Lee MJ, Lee JH, Rubinsztein DC (2013) Tau degradation: the ubiquitin-proteasome system versus the autophagy-lysosome system. Prog Neurobiol 105:49–59. https://doi.org/10.1016/j.pneurobio.2013.03.001
48. Cataldo AM, Peterhoff CM, Schmidt SD, Terio NB, Duff K, Beard M, Mathews PM, Nixon RA (2004) Presenilin mutations in familial Alzheimer disease and transgenic mouse models accelerate neuronal lysosomal pathology. J Neuropathol Exp Neurol 63:821–830. https://doi.org/10.1093/jnen/63.8.821
49. Chong CM, Ke M, Tan Y, Huang Z, Zhang K, Ai N, Ge W, Qin D, Lu JH, Su H (2018) Presenilin 1 deficiency suppresses autophagy in human neural stem cells through reducing γ-secretase-independent ERK/CREB signaling. Cell Death Dis 9:879. https://doi.org/10.1038/s41419-018-0945-7
50. Dobrowolski R, Vick P, Ploper D, Gumper I, Snitkin H, Sabatini DD, De Robertis EM (2012) Presenilin deficiency or lysosomal inhibition enhances Wnt signaling through relocalization of GSK3 to the late-endosomal compartment. Cell Rep 2:1316–1328. https://doi.org/10.1016/j.celrep.2012.09.026
51. Fedeli C, Filadi R, Rossi A, Mammucari C, Pizzo P (2019) PSEN2 (presenilin 2) mutants linked to familial Alzheimer disease impair autophagy by altering Ca(2+) homeostasis. Autophagy 15:2044–2062. https://doi.org/10.1080/15548627.2019.1596489
52. Hung COY, Livesey FJ (2018) Altered γ-secretase processing of APP disrupts lysosome and autophagosome function in monogenic Alzheimer's disease. Cell Rep 25:3647–3660 e3642. https://doi.org/10.1016/j.celrep.2018.11.095
53. Lee JH, Yu WH, Kumar A, Lee S, Mohan PS, Peterhoff CM, Wolfe DM, Martinez-Vicente M, Massey AC, Sovak G (2010) Lysosomal proteolysis and autophagy require presenilin 1 and are disrupted by Alzheimer-related PS1 mutations. Cell 141:1146–1158. https://doi.org/10.1016/j.cell.2010.05.008
54. Martín-Maestro P, Gargini R, Garcia AAS, Anton E, Noggle LC, Arancio S, Avila O, Garcia-Escudero J V (2017) Mitophagy failure in fibroblasts and iPSC-derived neurons of Alzheimer's disease-associated presenilin 1 mutation. Front Mol Neurosci 10:291. https://doi.org/10.3389/fnmol.2017.00291
55. Neely KM, Green KN, LaFerla FM (2011) Presenilin is necessary for efficient proteolysis through the autophagy-lysosome system in a γ-secretase-independent manner. J Neurosci 31:2781–2791. https://doi.org/10.1523/JNEUROSCI.5156-10.2010
56. Reddy K, Cusack CL, Nnah IC, Khayati K, Saqcena C, Huynh TB, Noggle SA, Ballabio A, Dobrowolski R (2016) Dysregulation of nutrient sensing and CLEARance in presenilin deficiency. Cell Rep 14:2166–2179. https://doi.org/10.1016/j.celrep.2016.02.006
57. Oikawa N, Walter J (2019) Presenilins and γ-secretase in membrane proteostasis. Cells 8:209. https://doi.org/10.3390/cells8030209
58. Kovacs GG, Gelpi E (2012) Clinical neuropathology practice news 3-2012: the ABC in AD-revised and updated guideline for the neuropathologic assessment of Alzheimer's disease. Clin Neuropathol 31:116–118. https://doi.org/10.5414/np300512
59. Yoshiyama Y, Higuchi M, Zhang B, Huang SM, Iwata N, Saido TC, Maeda J, Suhara T, Trojanowski JQ, Lee VM (2007) Synapse loss and microglial

activation precede tangles in a P301S tauopathy mouse model. Neuron 53:337–351. https://doi.org/10.1016/j.neuron.2007.01.010
60. Watanabe H, Smith MJ, Heilig E, Beglopoulos V, Kelleher RJ, Shen J (2009) Indirect regulation of presenilins in CREB-mediated transcription. J Biol Chem 284:13705–13713. https://doi.org/10.1074/jbc.M809168200
61. Diaz-Guerra E, Oria-Muriel MA, Moreno-Jimenez EP, de Rojasb I, Rodriguez C, Rodriguez-Traver E, Orera M, Hernandezb I, Ruizb A, Vicario C (2019) Generation of an integration-free iPSC line, ICCSICi006-A, derived from a male Alzheimer's disease patient carrying the PSEN1-G206D mutation. Stem Cell Res 40:101574. https://doi.org/10.1016/j.scr.2019.101574
62. Rodriguez-Traver E, Diaz-Guerra E, Rodriguez C, Arenas F, Orera M, Kulisevsky J, Moratalla R, Vicario C (2020) A collection of three integration-free iPSCs derived from old male and female healthy subjects. Stem Cell Res 42:101663. https://doi.org/10.1016/j.scr.2019.101663
63. Bains H, Singh R (2021) Isolation of autophagic fractions from mouse liver for biochemical analyses. STAR Protoc 2:100730. https://doi.org/10.1016/j.xpro.2021.100730
64. Kuninaka N, Kawaguchi M, Ogawa M, Sato A, Arima K, Murayama S, Saito Y (2015) Simplification of the modified Gallyas method. Neuropathology 35:10–15. https://doi.org/10.1111/neup.12144
65. Buee Scherrer V, Hof PR, Buee L, Leveugle B, Vermersch P, Perl DP, Olanow CW, Delacourte A (1996) Hyperphosphorylated tau proteins differentiate corticobasal degeneration and Pick's disease. Acta Neuropathol 91:351–359. https://doi.org/10.1007/s004010050436
66. Delacourte A, Robitaille Y, Sergeant N, Buee L, Hof PR, Wattez A, Laroche-Cholette A, Mathieu J, Chagnon P, Gauvreau D (1996) Specific pathological tau protein variants characterize pick's disease. J Neuropathol Exp Neurol 55:159–168
67. Greenberg SG, Davies P (1990) A preparation of Alzheimer paired helical fialments that displays distinct tau proteins by polyacrylamide gel electrophoresis. Proceeds Natl Acad Sci United States Am 87:5827–5831
68. Lee VM-Y, Balin BJ, Otvos L, Trojanowski JQ (1991) A68. A major subunit of paired helical filaments and derivatized forms of normal tau. Science 251:675–678
69. Liu WJ, Ye L, Huang WF, Guo LJ, Xu ZG, Wu HL, Yang C, Liu HF (2016) p62 links the autophagy pathway and the ubiqutin-proteasome system upon ubiquitinated protein degradation. Cell Mol Biol Lett 21:29. https://doi.org/10.1186/s11658-016-0031-z
70. Mizushima N, Yoshimori T, Levine B (2010) Methods in mammalian autophagy research. Cell 140:313–326. https://doi.org/10.1016/j.cell.2010.01.028
71. Mauthe M, Orhon I, Rocchi C, Zhou X, Luhr M, Hijlkema KJ, Coppes RP, Engedal N, Mari M, Reggiori F (2018) Chloroquine inhibits autophagic flux by decreasing autophagosome-lysosome fusion. Autophagy 14:1435–1455. https://doi.org/10.1080/15548627.2018.1474314
72. Wulansari N, Darsono WHW, Woo HJ, Chang MY, Kim J, Bae EJ, Sun W, Lee JH, Cho IJ, Shin H et al (2021) Neurodevelopmental defects and neurodegenerative phenotypes in human brain organoids carrying Parkinson's disease-linked DNAJC6 mutations. Sci Adv 7:eabb1540. https://doi.org/10.1126/sciadv.abb1540
73. Lasagna-Reeves CA, Castillo-Carranza DL, Guerrero-Muoz MJ, Jackson GR, Kayed R (2010) Preparation and characterization of neurotoxic tau oligomers. Biochemistry 49:10039–10041. https://doi.org/10.1021/bi1016233
74. Patterson KR, Remmers C, Fu Y, Brooker S, Kanaan NM, Vana L, Ward S, Reyes JF, Philibert K, Glucksman MJet al et al (2011) Characterization of prefibrillar Tau oligomers in vitro and in Alzheimer disease. J Biol Chem 286:23063–23076. https://doi.org/10.1074/jbc.M111.237974
75. Coffey EE, Beckel JM, Laties AM, Mitchell CH (2014) Lysosomal alkalization and dysfunction in human fibroblasts with the Alzheimer's disease-linked presenilin 1 A246E mutation can be reversed with cAMP. Neuroscience 263:111–124. https://doi.org/10.1016/j.neuroscience.2014.01.001
76. Costa-Laparra I, Juarez-Escoto E, Vicario C, Moratalla R, Garcia-Sanz P (2023) APOE epsilon4 allele, along with G206D-PSEN1 mutation, alters mitochondrial networks and their degradation in Alzheimer's disease. Front Aging Neurosci 15:1087072. https://doi.org/10.3389/fnagi.2023.1087072
77. Tang Z, Bereczki E, Zhang H, Wang S, Li C, Ji X, Branca RM, Lehtio J, Guan Z, Filipcik Pet al et al (2013) Mammalian target of rapamycin (mTor) mediates tau protein dyshomeostasis: implication for Alzheimer disease. J Biol Chem 288:15556–15570. https://doi.org/10.1074/jbc.M112.435123
78. Ryu HY, Kim LE, Jeong H, Yeo BK, Lee JW, Nam H, Ha S, An HK, Park H, Jung S al (2021) GSK3B induces autophagy by phosphorylating ULK1. Exp Mol Med 53:369–383. https://doi.org/10.1038/s12276-021-00570-6
79. Xu D, Shan B, Lee BH, Zhu K, Zhang T, Sun H, Liu M, Shi L, Liang W, Qian et al (2015) L Phosphorylation and activation of ubiquitin-specific protease-14 by Akt regulates the ubiquitin-proteasome system. Elife 4:e10510 https://doi.org/10.7554/eLife.10510
80. Kim E, Park S, Lee JH, Mun JY, Choi WH, Yun Y, Lee J, Kim JH, Kang MJ, Lee MJ (2018) Dual function of USP14 deubiquitinase in cellular proteasomal activity and autophagic flux. Cell Rep 24:732–743. https://doi.org/10.1016/j.celrep.2018.06.058
81. Wei Z, Zeng K, Hu J, Li X, Huang F, Zhang B, Wang JZ, Liu R, Li HL, Wang X (2022) USP10 deubiquitinates tau, mediating its aggregation. Cell Death Dis 13:726. https://doi.org/10.1038/s41419-022-05170-4
82. Aulston B, Liu Q, Mante M, Florio J, Rissman RA, Yuan SH (2019) Extracellular vesicles isolated from familial Alzheimer's disease neuronal cultures induce aberrant Tau phosphorylation in the wild-type mouse brain. J Alzheimers Dis 72:575–585. https://doi.org/10.3233/JAD-190656
83. Podvin S, Jones A, Liu Q, Aulston B, Mosier C, Ames J, Winston C, Lietz CB, Jiang Z, O'Donoghue AJet al et al (2021) Mutant presenilin 1 dysregulates exosomal proteome cargo produced by human-induced pluripotent stem cell neurons. ACS Omega 6:13033–13056. https://doi.org/10.1021/acsomega.1c00660
84. Khurana V, Elson-Schwab I, Fulga TA, Sharp KA, Loewen CA, Mulkearns E, Tyynela J, Scherzer CR, Feany MB (2010) Lysosomal dysfunction promotes cleavage and neurotoxicity of tau in vivo. PLoS Genet 6:e1001026. https://doi.org/10.1371/journal.pgen.1001026
85. Letronne F, Laumet G, Ayral AM, Chapuis J, Demiautte F, Laga M, Vandenberghe ME, Malmanche N, Leroux F, Eysert F et al (2016) ADAM30 downregulates APP-linked defects through cathepsin D activation in Alzheimer's disease. eBioMedicine 9:278–292. https://doi.org/10.1016/j.ebiom.2016.06.002
86. Amritraj A, Wang Y, Revett TJ, Vergote D, Westaway D, Kar S (2013) Role of cathepsin D in U18666A-induced neuronal cell death: potential implication in Niemann-Pick type C disease pathogenesis. J Biol Chem 288:3136–3152. https://doi.org/10.1074/jbc.M112.412460
87. Almeida MC, Eger SJ, He C, Audouard M, Nikitina A, Glasauer SMK, Han D, Mejia-Cupajita B, Acosta-Uribe J, Villalba-Moreno ND (2024) Single-nucleus RNA sequencing demonstrates an autosomal dominant Alzheimer's disease profile and possible mechanisms of disease protection. Neuron 112:1778–1794 e1777. https://doi.org/10.1016/j.neuron.2024.02.009

Publisher's note